

**Dynamic Simulation Methods for Evaluating
Motor Vehicle and Roadway Design and
Resolving Policy Issues**

J.W. Stoner

Associate Professor, Civil and Environmental Engineering

M.A. Bhatti

Associate Professor, Civil and Environmental Engineering

S.S. Kim

Assistant Professor, Mechanical Engineering

J.K. Koo

Mechanical Engineering

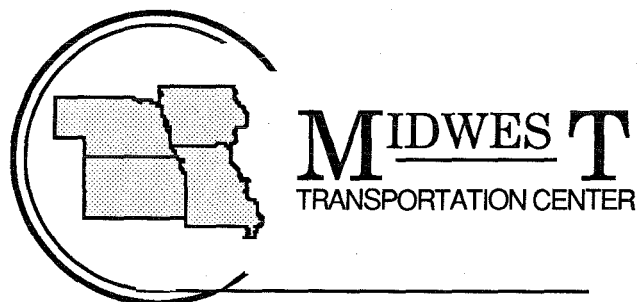
I. Molinas-Vega

Civil and Environmental Engineering

B. Amhof

Civil and Environmental Engineering

January, 1990



This study was funded by the University Transportation Centers Program of the U.S. Department of Transportation, and the Iowa Department of Transportation. The results and views expressed are the independent products of university research and are not necessarily concurred in by the funding agencies.

Public Policy Center
227 South Quadrangle
University of Iowa
Iowa City, IA 52242
Phone: (319) 335-6800
Fax: (319) 335-6801

PREFACE

This report is the product of a first-year research project in the University Transportation Centers Program. The Program was created by Congress in 1987 to “contribute to the solution of important regional and national transportation problems.” A university-based center was established in each of the ten federal regions following a national competition in 1988. Each center has a unique theme and research purpose, although all are interdisciplinary and also have educational missions.

The Midwest Transportation Center is one of the ten centers; it is a consortium that includes Iowa State University (lead institution) and The University of Iowa. The Center serves federal Region 7 which includes Iowa, Kansas, Missouri, and Nebraska. Its theme is “transportation actions and strategies in a region undergoing major social and economic transition.” Research projects conducted through the Center bring together the collective talents of faculty, staff, and students within the region to address issues related to this important theme.

This particular project was carried out by an interdisciplinary research team at The University of Iowa’s Public Policy Center. This center is a reflection of the University’s renewed commitment to applied research that seeks to advance the public interest. The Center’s projects generally involve close interaction with decision makers and resource people in both the public and private sectors.

The project is central to the Midwest Transportation Center’s theme in that it examines the relationship between road highway design and allowable truck axle weights and configurations. The principal investigator was Professor James W. Stoner, Civil and Environmental Engineering. Co-investigators were Professors Sang Sup Kim, Mechanical Engineering and Asghar Bhatti, Civil and Environmental Engineering. They were assisted by Jakyum Koo and Idelin Molinas-Vega, graduate students in Engineering, and Bryce Amhof and Jason Fabritz, undergraduate students in Civil and Environmental Engineering. Support services for computing were provided by the Center for Simulation and Design Optimization at the University of Iowa, under the direction of Dr. Ed Haug.

ACKNOWLEDGMENTS

The research and development performed during the first year of this project required the assistance of many people. The Project Advisory Committee satisfied many of our critical data needs, assisted in the preparation of our work program, and reviewed our drafts of this report. Members of the Advisory Committee included Bill McCall and Brian McWaters of the Iowa Department of Transportation; Bill Giles of the Ruan Companies; and Charley Powell of Navistar. In addition, staff members at the Iowa Department of Transportation provided advice and data, specifically Charlie Potter and Samil Sermet. Kurt Smith and Mike Darter of ERES Consulting provided data on pavement deformation and thickness design using the results of finite element analysis.

The University Transportation Centers Program of the U.S. Department of Transportation deserves our thanks for making it possible to carry out this research. Also, Professor Allen and his colleagues at Iowa State University provided direction and administrative guidance that helped us through the first year.

Terri Bell and Sylvia Huerta typed the report and provided production support throughout the project, while our other associates at the Public Policy Center assisted us in numerous ways. We thank them all.

TABLE OF CONTENTS

PREFACE	ii
ACKNOWLEDGMENTS.....	iii
TABLES	v
FIGURES	vi
SUMMARY OF FIRST YEAR PROGRESS.....	1
Variable Specification	1
Data Analysis and Verification.....	2
RELATIONSHIPS TO PREVIOUS RESEARCH	2
Vehicle Load History Studies.....	2
Pavement Analysis	3
VEHICLE MODELING AND DYNAMIC LOAD ESTIMATION.....	5
Vehicle Specification	6
Two Dimensional Vehicle Model.....	6
Simulation Results and Discussion	13
Dynamic Load Effects of a Slab Fault as a Function of Speed	14
Dynamic Load Effects of Continuous Slab Warping	14
Three-Dimensional Model.....	23
FINITE ELEMENT ANALYSIS OF RIGID PAVEMENTS	25
Modeling Procedures.....	25
Pavement Response Analysis Procedure.....	34
Vehicle and Pavement Models for Parametric Studies.....	36
Results of the Parametric Studies.....	36
RESEARCH DISCUSSION.....	57
Summary of First-Year Findings.....	57
Further Research Needs.....	58
Proposed Research Extensions and Second Year Work Plan.....	59
REFERENCES.....	61
APPENDIX 1.....	62

TABLES

Table 1	Vibration Modes of a Tractor/Semitrailer	14
Table 2	Axles Causing Maximum Deflections at Different Locations and Different Road Conditions.....	56

FIGURES

Figure 1	Typical Single and Tandem Axle Configurations	7
Figure 2	Three Common Tandem Axle Designs.....	8
Figure 3	Geometric Configuration of Tractor/Semitrailer Combination.....	10
Figure 4	Tandem Leaf Spring Suspension for Two Dimensional Model.....	10
Figure 5	Envelope of Leaf Spring Response.....	12
Figure 6	Comparison of Full and Simple Simulation Model Dynamic Load Estimates for Front Axle Hitting a Bump at 30 MPH.....	15
Figure 7	Dynamic Load for the Steering Axle (half inch faulting)	16
Figure 8	Pitch Angle of Tractor and Semitrailer (half inch faulting and 65 mph)	16
Figure 9	Dynamic Load for the Leading Axle of Tractor Tandem (half inch faulting)	17
Figure 10	Dynamic Load for the Trailing Axle of Tractor Tandem (half inch faulting)	17
Figure 11	Dynamic Load for the Leading Axle of Trailer Tandem (half inch faulting)	18
Figure 12	Dynamic Load for the Trailing Axle of Trailer Tandem (half inch faulting)	18
Figure 13	Aggregate Dynamic Load for Continuous Slab Warping (20 ft. slab length)	20
Figure 14	Dynamic Wheel Loads for each Axle for Continuous Slab Warping (30 mph and 20 ft. slab)	20
Figure 15	Dynamic Wheel Load for Each Axle for Continuous Slab Warping (45 mph and 20 ft. slab)	21
Figure 16	Dynamic Wheel Loads for Each Axle for Continuous Slab Warping (65 mph and 25 ft. slab)	21
Figure 17	Approach Profile for Instrumented Test Segment.....	22
Figure 18	Aggregate Dynamic Load Coefficient for Instrumented Test Pavement at 30 and 65 mph	22
Figure 19	Representation of Winkler and Elastic Subgrades	26
Figure 20	ANSYS/STIF91 Eight Node Layered Shell	27

Figure 21	Springs Location for STIF91 and Influence Areas	28
Figure 22	Mesh Layout and Material Properties for Example 1 Chou (1981).....	30
Figure 23	Mesh Layout Used by Chou (1981).....	31
Figure 24	Comparison of WESLIQID Finite Solution with Westergaard's Solution, deflections (Chou, 1981).....	32
Figure 25	Slab Cross Section with Material Characteristics	33
Figure 26	Nodal Array to Finite Model.....	35
Figure 27	Nodal Response Matrix	35
Figure 28	Pavement Model for Parametric Study	37
Figure 29a	Dynamic Wheel Path Load for Steering Axle (half inch bump)	39
Figure 29b	Dynamic Wheel Load for Leading Axle of Trailer Tandem (half inch bump)	39
Figure 29c	Dynamic Wheel Path Load for Trailing Axle of Tractor Tandem (half inch bump)	39
Figure 29d	Dynamic Wheel Path Load for Leading Axle of Semitrailer Tandem (half inch bump)	40
Figure 29e	Dynamic Wheel Path Load for Trailing Axle of Semitrailer Tandem (half inch bump)	40
Figure 30	Envelope of Maximum Slab Displacement for Bump Case.....	41
Figure 31a	Dynamic Wheel Path Load for Steering Axle (half inch fault).....	42
Figure 31b	Dynamic Wheel Path Load for Leading Axle of Tractor Tandem (half inch fault).....	42
Figure 31c	Dynamic Wheel Path Load for Trailing Axle of Tractor Tandem (half inch fault).....	42
Figure 31d	Dynamic Wheel Path Load for Leading Axle of Semitrailer Tandem (half inch fault).....	43
Figure 31e	Dynamic Wheel Path Load for Trailing Axle of Semitrailer Tandem (half inch fault).....	43
Figure 32	Envelope of Maximum Slab Displacement for Faulting Case	44
Figure 33a	Dynamic Wheel Path Load for Steering Axle (continuous faulting)	46

Figure 33b	Dynamic Wheel Path Load for Leading Axle of Tractor Tandem (continuous faulting)	46
Figure 33c	Dynamic Wheel Path Load for Trailing Axle of Tractor Tandem (continuous faulting)	46
Figure 33d	Dynamic Wheel Path Load for Leading Axle of Semitrailer Tandem (continuous faulting)	47
Figure 33e	Dynamic Wheel Path Load for Trailing Axle of Semitrailer Tandem (continuous faulting)	47
Figure 34	Envelope of Maximum Slab Displacements for Continuous Faulting Case.....	48
Figure 35	Envelope of Maximum Slab Displacements for Moving Static Load	48
Figure 36a	Dynamic Wheel Path Load for Steering Axle (continuous warping)	49
Figure 36b	Dynamic Wheel Path Load for Leading Axle of Tractor Tandem (continuous warping).....	49
Figure 36c	Dynamic Wheel Path Load for Trailing Axle of Tractor Tandem (continuous warping).....	49
Figure 36d	Dynamic Wheel Path Load for Leading Axle of Semitrailer Tandem (continuous warping).....	50
Figure 36e	Dynamic Wheel Path Load for Trailing Axle of Semitrailer Tandem (continuous warping).....	50
Figure 37	Envelope of Maximum Slab Displacements for Continuous Warp Case....	51
Figure 38	Pay Load Effect of Trailer on Slab Displacement Envelope	51
Figure 39a	Dynamic Wheel Path Load for Steering Axle (real profile).....	53
Figure 39b	Dynamic Wheel Path Load for Leading Axle of Tractor Tandem (real profile)	53
Figure 39c	Dynamic Wheel Path Load for Trailing Axle of Tractor Tandem (real profile)	53
Figure 39d	Dynamic Wheel Path Load for Leading Axle of Semitrailer Tandem (real profile)	54
Figure 39e	Dynamic Wheel Path Load for Trailing Axle of Semitrailer Tandem (real profile)	54
Figure 40	Envelope of Maximum Slab Displacements for Real Profile Case.....	55

DYNAMIC SIMULATION METHODS FOR EVALUATING MOTOR VEHICLE AND ROADWAY DESIGN AND RESOLVING POLICY ISSUES

Interim Report

SUMMARY OF FIRST YEAR PROGRESS

There are three primary objectives of this study. The first is to develop a comprehensive truck simulation that executes rapidly, has a modular program construction to allow variation of vehicle characteristics, and is able to realistically predict vehicle motion and the tire-road surface interaction forces. A second is to develop a model of doweled Portland Cement Concrete pavement that can be used to determine slab deflection and stress at predetermined nodes. The pavement model must allow for the variation of traditional thickness design factors. Finally, the two models should be implemented on a work station with suitable menu driven modules so that both existing and proposed pavements can be evaluated with respect to design life, given specific characteristics of the heavy vehicles that will be using the facility. This system would assist the Departments of Transportation in their evaluation of maintenance procedures, and the determination of appropriate performance standards for urban and rural highway segments and commercial highway networks. This report summarizes the work that has been performed during the first year of this study.

A two dimensional model of a typical 3-S2 tractor-trailer combination was created using the DADS code for simulating dynamic mechanical systems. Load histories for the vehicle were estimated in the wheel path for a sequence of doweled portland cement concrete slabs defined by the specification for an actual instrumented pavement segment on Interstate 80 in western Iowa. The specifications for the axle, tires, suspension, drive train, and the dimensions and structural descriptions of the vehicle components were obtained from manufacturer's data. A finite element structural analysis program, ANSYS, was used to model the pavement to allow estimation of strains and displacements within the slab and at the doweled joints. The model was validated using results obtained from other finite element codes.

Data from the instrumented slab will eventually be used to compare observed load and displacement profiles with the computer model results. A weigh-in-motion system is also in place both before and after the instrumented slabs to allow an estimation of dynamic loads relative to known static loads.

Computer runs have been performed varying the parameters defining both vehicle and road elements. For the vehicle, these include speed, weight and weight distribution, suspension type, tire pressures, and load leveling capability of the suspension. For the roadway, the sensitivity of results is related to road roughness, bumps or faults at the joints, soil support values, slab warp and curl, and load distribution and concurrent displacement induced by the vehicle passing over the slabs.

The resulting time specific displacements for each node are plotted, and the displacement basin is generated for defined vehicles. Relative damage to the pavement can then be estimated. A damage function resulting from load replications must be assumed that will be reflected by further

pavement deterioration. Comparison with actual damage on Interstate 80 will eventually allow verification of the above procedures.

Variable Specification

The modeling process can be viewed from the perspective of both the vehicle and the roadway. The variables and the modeling procedures are different, but there is always interaction between the two. The tractor-trailer combination generates wheel load force histories from both the sprung and unsprung vehicle mass as it moves down the highway. The variables affecting the magnitude of the dynamic load include the vehicle characteristics such as axle load, load distribution; suspension type, design and condition; tire stiffness; axle spacing and load leveling; and tire and wheel configuration. Operating conditions such as vehicle speed, road surface roughness and irregularities, geometric design of the roadway, and even environmental conditions can have significant influence.

The rigid pavement suffers some displacement as the load is applied through normal tire forces on the surface. The load is distributed and transferred to the subgrade and soil, whose support value is determined by soil or aggregate type and modified by the soil stabilization, temperature and moisture content. The properties of the concrete include the modulus of rupture, thickness, and load transfer efficiencies at the longitudinal and transverse joints. The slab may contain surface deformities and warp and curl induced by the natural curing process or internal temperature differences. Displacement also occurs during the traversing of the axle loads, causing some deformation and skewing of the slab. The ability of the slab to distribute and accommodate load is often a function of the cracking, faulting, and other damage resulting from cumulative repetitions of axle loads.

Data Analysis and Verification

The instrumented pavement segment on Interstate-80 near Avoca, Iowa, consists of two twenty foot slabs with skewed doweled transverse joints. The instrumentation consists of 50 sensors to measure displacement of the dowels in the wheel path at the entry and leaving points of the segment and at all dowels on the first slab in the outside lane. Strain gauges are located at mid-slab locations. Sixteen deflection sensors are located at various points in the two slabs, but primarily in the anticipated wheel paths. Temperature and moisture content sensors are located in the sub-grade to estimate the soil support values during specific data collection intervals.

In addition, data will be collected simultaneously from two weigh-in-motion locations both before and after the instrumented slab. The weigh-in-motion data will include estimated dynamic weights, estimates of speed, wheel path location, and axle spacing.

This data set will allow verification of the pavement model, not necessarily in exact magnitude, but in terms of calculating the influence profile at a specific node and the deflection basin resulting from the passage of a specific vehicle. The strain and deflection readings are in volts, so the combined weigh-in-motion and pavement model results will allow scaling of pavement displacement and internal forces. The life expectancy of the various sensors is

unknown, but a continuing data collection effort will provide an analysis of sensitivity to changes in weather and consumption of the design life of the pavement.

RELATIONSHIPS TO PREVIOUS RESEARCH

Vehicle Load History Studies

Modeling of different truck configurations has been performed by different researchers throughout the world, but there are three research groups currently working with computer models of heavy vehicles to predict dynamic loads; UMTRI at the University of Michigan, the Massachusetts Institute of Technology, and CCAD at the University of Iowa. Other research has measured normal forces produced by vehicles using instruments implanted in or placed on the roadway, shaker tables under actual vehicles, and instrumented truck axles.

The dynamic loads are usually typified by two statistics, the dynamic load coefficient, which is the standard deviation of the dynamic load divided by the static load, and the peak load or impact factor.

Dynamic load is a significant component of the total force, but obviously, what goes up must come down, so the peak forces are distributed along the wheel path according to the wave forms that are produced by the frequencies excited by the road roughness or non-uniformities encountered in the road profile.

Smooth roads produce very small values of the Dynamic Load Coefficient (DLC), but even on relatively good roads, there is a significant difference in the performance of differing suspension designs. Walking beam suspensions are the worst, while air bags are the best with DLC's roughly half the walking beam values, and leaf springs are somewhere in the middle, the value depending on the spring stiffness and axle spacing.

There is some difference of opinion concerning the impact of tire pressure, although in general tire pressures do not have a significant effect; they only increase the total axle loads a small amount, 5.5% for 125 psi vs 75 psi. The change in the contact patch and tire stiffness would cause considerable difference in the contact pressures on the pavement, a factor that could have considerable influence on flexible pavements. There is little impact for rigid pavement because of the shape of the influence function due to the bridging capability of the material.

Vehicle speed is an important factor, both in magnitude of the peak forces and the point at which the maximum forces impact on the slab. At low speeds, dynamic contributions are minimal and the resulting forces are much like static load. There are critical mid-range speeds, 45-60 mph where the specific vehicle and pavement characteristics combine to maximize tire forces. At higher speeds, the overall dynamic forces are reduced, but extremely rough pavement could excite some of the suspension modes and produce increased dynamic loads.

Pavement Analysis

Numerous analyses using several mathematical analysis procedures have been performed on strains and deflections in pavement caused by the passage of heavy vehicles. Instrumented pavements have been used to gather experimental data and complex finite element codes have been used to represent both rigid and flexible pavement layers. Flexible pavement is significantly different in terms of its response to load because of both the nature of the materials and the shape of the influence pattern, but both flexible and rigid pavements must eventually distribute the loads to the prepared subgrade and soil layers. A number of references describe traditional thickness design procedures and the analysis of strains, temperature differentials, deformation, and consequent damage to pavements. This interim study is concerned only with the response of rigid PPC pavement of the types typically found in Iowa.

A common measurement of stress is the deflection induced at specific points in the roadway. An attempt to summarize the effect of loads on pavement is the road stress factor, which is the fourth power of the ratio of the peak force at a point to the mean force, or static load although this variable has been seriously questioned in recent studies. There is considerable variation in the loads across the slab wheel path. The most conservative studies estimate at least a 25% point to point variation. The load pattern and the variation in load is determined by the variation in the road profile, or, to some degree, the relative road roughness.

Previous studies have shown that the height of a joint fault or bump is directly related to the magnitude of the peak load or impact force but it does not affect the relative location of impact. The increase in magnitude appears to be a power function of the height of the deformation. Slab warp has been found to have considerable influence on both location and magnitude of peak loads. The determining factors are slab length, deflection and slab radius of curvature, vehicle speed, and axle spacing and configuration. Overall low levels of slab roughness seems to have little effect on the dynamic loads. The primary factor in excitation of the vehicle modes were the deformations at rigid pavement joints.

The response of the pavement in terms of deflection and eventual plastic deformation of the subgrade, is related to the bearing capacity or support value of the stabilized or natural base. As previously stated, this can be a function of many climatic and environmental characteristics.

VEHICLE MODELING AND DYNAMIC LOAD ESTIMATION

Irregularities in the road surface impose continuously varying displacements at the points of contact between a vehicle's tires and the road surface. As a result, the normal wheel forces fluctuate about the static load levels. The peak magnitude of this dynamic load may be much greater than the measured static axle load. The instantaneous dynamic load is accompanied by large dynamic stresses and strains in the road surface, having significant impact on pavement performance.

Recent studies [1-4] have established that the dynamic wheel loads of a moving vehicle depend primarily on vehicle speed, level of pavement roughness, and axle and suspension characteristics. Sayers and Gillespie [1] measured dynamic loads for three suspension types on varying road roughnesses, to investigate the relationship between the observed dynamic loads and design features of the tandem suspensions. With the aid of a relatively simple computer model with three degrees of freedom, the research provides a good understanding of the nature of the vibratory modes that effect dynamic wheel loading.

Markow, Hedrick et al [2] developed an analytical model of vehicle pavement interaction that links a simple vehicle model with a pavement response model. The most significant finding was that the pavement damage caused by a leaf spring type suspension is strongly dependent on the degree of damping provided by interleaf friction. Greater damping generally leads to significantly lower damage. Pavement cracking failure for flexible pavement is shown to be highly sensitive to tire pressure - 120 PSI pressure is twice as damaging as 75 PSI. The walking beam was found to be the most damaging suspension type due to its relatively undamped axle coupling. As expected the air bag suspension was found to be the least damaging.

Cebon [3,4] provided a nonlinear and linear time domain analysis technique for the mathematical vehicle model and generated several criteria for relating dynamic forces to road surface damage. The insight offered by his study is the recognition that the dynamic loads imposed by a vehicle do not randomly distribute themselves over the road, but tend to localize in specific areas of pavement. The peak dynamic loads that result in the most damage would occur repeatedly in the same general locations, thus reducing serviceability by accelerating degradation of specific sections of pavement. Time histories of wheel force were generated using random road profiles as input to a vehicle dynamics model with six degrees of freedom. He computed aggregate force, defined as the distribution of individual wheel loads experienced by discrete segments of pavement. It was found that 5% of the surface area of the road is subjected to aggregate force levels greater than the 95th percentile overall aggregate force.

Most of the documented studies have used a linear vehicle model or a quite simplified nonlinear vehicle model to determine the interaction between vehicle and pavement due to generic changes in vehicle suspension parameters, vehicle speed, and road characteristics. While such analyses provide an inexpensive and convenient solution that has yielded a good deal of insight into the vehicle and pavement interaction, they have limitations in their ability to accommodate a wide range of vehicle configurations and vehicle operations.

Vehicle/pavement interaction depends on a large number of vehicle configurations and resulting mass distributions, axle spacing and configuration, and suspension and tire characteristics. For accurate prediction of dynamic loading on the pavement surface, a comprehensive state-of-art model of truck dynamic behavior must be applied to evaluate the effect of changes in vehicle characteristics on the forces that are significant for pavement performance.

One of the major objectives of this study is to develop a comprehensive truck simulation model that provides real vehicle response and yet is flexible enough to include dynamic interactions between various components of the vehicle for realistically predicting vehicle motion and tire-road surface interaction force. To achieve this goal, we used a mechanical system dynamics approach for vehicle modeling and simulation.

Vehicle Specification

Truck configurations can be divided into four major categories; five-axle tractor-semitrailer (3S2), three-axle tractor-semitrailer (2S1), five-axle double (2S1-2), and seven-axle triple (2S1-2-2). The five-axle tractor-semitrailer is the most widely used truck configuration covering about 60% of the tractor-trailer population. These heavy truck combinations are composed of three vehicle units of tractor, semitrailer, and dolly. Each unit is connected by fifth wheel or a hitch mechanism. The major components of the vehicle unit are chassis, axle groups, suspensions, and tires. An excellent review of heavy truck characteristics for pavement interaction is given in Ref. [6].

Axles are typically described as being single or tandem. The single axle, shown in Figure 1, can be mounted on a tractor or a trailer, and may be a driving or a load carrying axle. The front steering axle is always a single axle.

The basic principle of a tandem axle, also shown in Figure 1, is that the load is evenly distributed to both axles, however, there are certain cases where an uneven load distribution is maintained but always with the same ratio. In reality this equalization does not always work well. The three major suspension types for the tandem axle are the four-leaf spring, air bag, and walking beam suspensions as shown in Figure 2.

Two Dimensional Vehicle Model

The DADS computer code builds a mathematical model of the real system that calculates position, velocity, and acceleration of the various parts of the vehicle, as well as resultant forces that act in the system. In the two dimensional model, each body in a vehicle is described by three generalized coordinates for its location and orientation of a body-fixed reference frame.

As joints or other constraints are added connecting the various bodies of the vehicle system, some degrees of freedom for the connected bodies are removed, limiting their relative motion as prescribed by the particular joints or constraints.

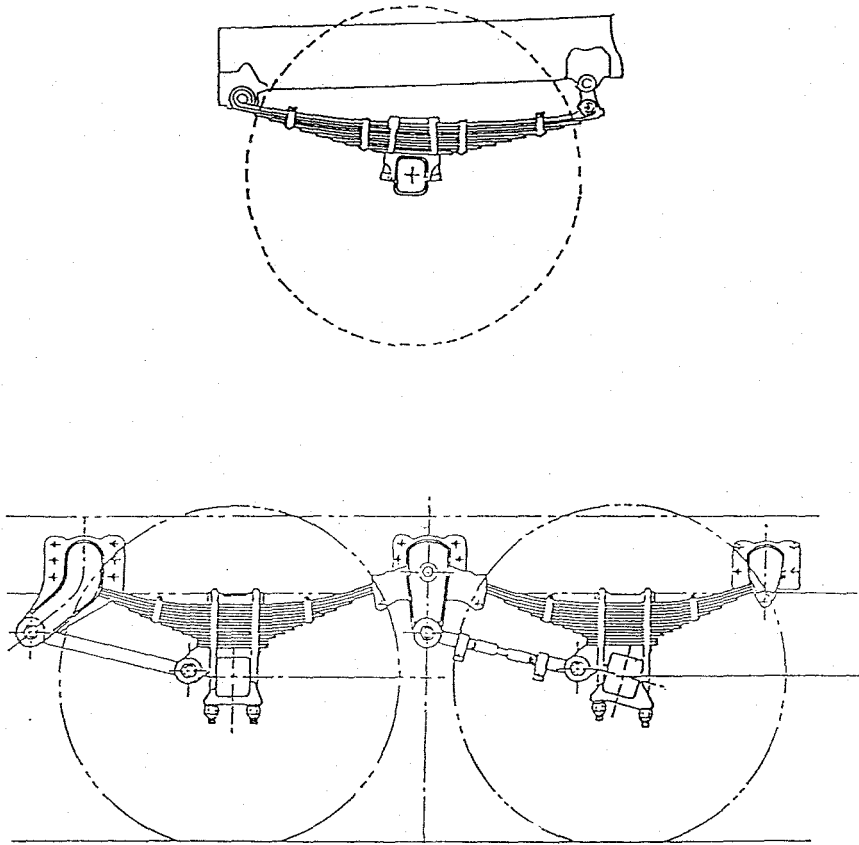


Figure 1
Typical Single and Tandem Axle Configurations

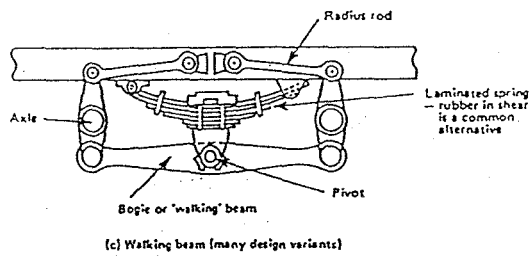
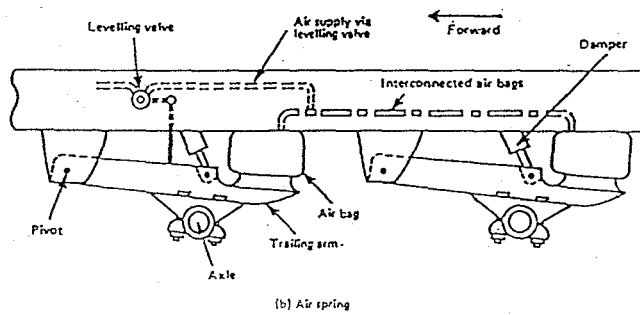
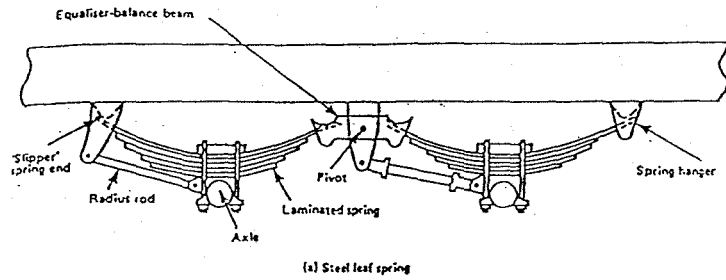


Figure 2
Three Common Tandem Axle Designs

When a vehicle model has been completely defined, the total number of generalized coordinates of the bodies minus the number of independent constraint equations for joints and constraints, yields the number of degrees of freedom present in the system.

Once a vehicle model has been defined from the library, the data set is processed by the DADS analysis program and the model is mathematically assembled. The equations of the motion for each body of the vehicle, are automatically generated and numerically solved.

Results of the vehicle simulation are in terms of positions, velocities, and accelerations of each body. Also included are various data on any force elements in the model such as tire contact forces to the pavement, spring forces between chassis and suspension bodies, and if necessary, internal reaction forces due to any joints or constraints in the model. Having a good mathematical representation of the physical system of the vehicle is much more flexible than a conventional vehicle analysis tool. It is a simple process to change various specifications of either the model or the method of analysis. Furthermore, since DADS is structured as a combination of individually modulated subroutines, it becomes advantageous to attach the different suspension modules to the existing DADS code.

Tractor/Semitrailer model

The two dimensional articulated vehicle model used in this study is illustrated in Figure 3. The cab, engine, and tractor chassis are considered as one body; as is the semitrailer with its chassis. In order to keep the solution within a reasonable simulation solution time the following simplifying assumptions have been made.

- 1) The tractor and semitrailer are assumed to be rigid bodies.
- 2) The vehicle moves at constant speed.
- 3) The input to the articulated vehicle model during the simulation is the perturbation of the symmetric road profile through the tires.

The tractor and trailer are connected by a friction-free fifth wheel represented as a revolute joint. Due to the kinematic coupling at the fifth wheel, the bounce and pitch motion of the semitrailer will contribute to the dynamic loads produced by the tractor motion. The bodies of each suspension system are also connected to the truck and semitrailer by joints. The connectivity and DADS modelling is explained in the following section, while detailed geometric data and vehicle parameters of the truck/semitrailer are given in Appendix 1.

Four-Leaf Suspension Model

Two four-leaf spring elements are modeled in tandem axle suspension as shown in Fig. 4. In order to obtain load equalization, one side of the end of each spring is pinned to the load leveler linkage that is in turn connected to the chassis by revolute joint. By assuming that the pivot is friction free, the forces produced by the leaf spring are idealistically constrained to be equal. A massless torsion bar attached between the axle housing and the chassis by two revolute joints, restricts the relative horizontal motion of the axle and the chassis. Also, the solid axle is modeled as a 'single leaf' spring to connect to the tractor for translational motion. The simulation system

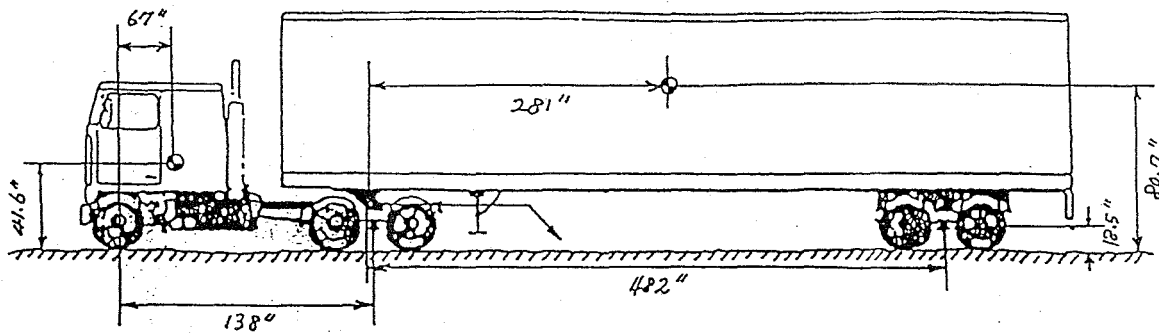


Figure 3
 Geometric Configuration of Tractor/Semitrailer Combination

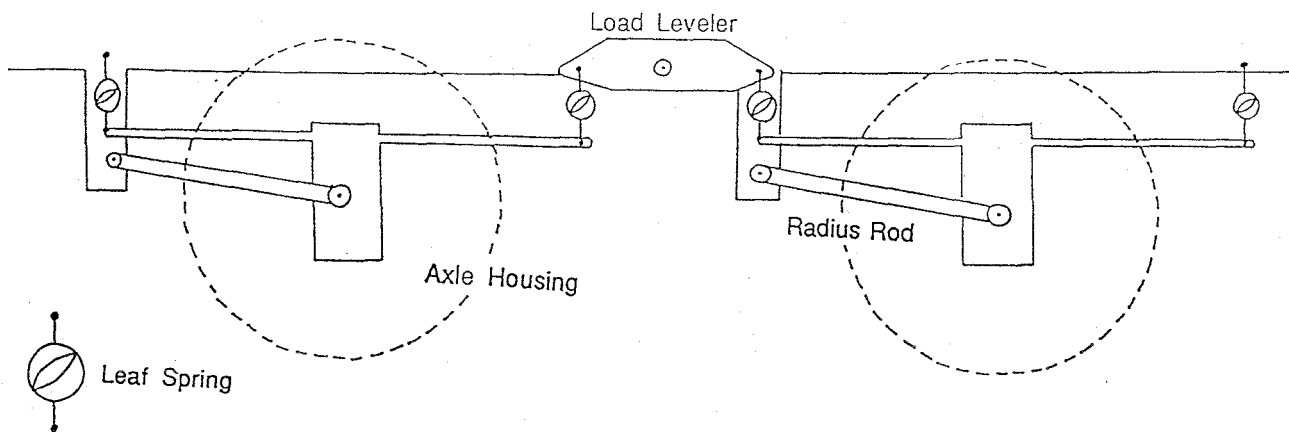


Figure 4
 Tandem Leaf Spring Suspension for Two Dimensional Model

handles these kinematic joints in the form of kinematic constraints between bodies and automatically produces the coupling motions between the suspension system and the chassis.

The goal of the leaf spring element is to calculate displacement at the attachment points and compute the force components. These forces are then applied to the bodies that are connected by the leaf springs, which control the relative vertical motion of both the sprung mass and unsprung mass. The leaf spring is a complex and nonlinear force/displacement device. Much of the complexity derives from the ability of the leaf spring to store and dissipate energy. Because of the hysteretic behavior of leaf spring, representation of the spring rate and friction levels as a constant is not valid for the dynamic load condition. Experimental data from leaf spring tests have shown that the vertical force within the leaf spring varies as a function of displacement and relative velocity. Figure 5 illustrates the typical hysteretic shape of the force versus deflection curves.

A model of these springs suitable for representing their characteristics over wide range of loading, deflection amplitude, and random reversals of velocity is desirable for dynamic load prediction. An extensive study of this behavior by the University of Michigan Transportation Research Institute (UMTRI) has yielded an equation to describe the force based experimental data. The equation developed by UMTRI at PHASE IV to describe this behavior is shown below.

$$F_i = F_{ENV_j} + (F_{i-1} - F_{ENV_j}) e^{-\left[\frac{\delta_i - \delta_{i-1}}{\beta_j} \right]}$$

where:

- F_i is the suspension force at the current simulation time step
- F_{i-1} is the suspension force at the last simulation time step
- δ_i is the suspension deflection at the current simulation i^{th} time
- δ_{i-1} is the suspension deflection at the last simulation time step ($i-1^{\text{th}}$ time step)
- F_{ENV_j} is the force corresponding to the upper and lower boundaries of the envelope of the measured spring characteristics at the deflection, δ_i .
- β_j is an input parameter used for describing the rate at which the suspension force within a hysteresis loop approaches the outer boundary of the envelope, F_{ENV_j} .

Implementation of this equation in the DADS leaf spring element requires accessing the curve data based on the parameters listed above. If the spring is in jounce moving toward the chassis, the upper curve is used as a boundary. The lower curve is used as a boundary when the spring is in rebound moving away from the chassis. The index j used in the equation indicates the two envelopes shown in Figure 5. Then, current displacement is saved for next time step as δ_{i-1} . The new vertical force value is used to replace the previously obtained component. The next step is to transform the forces and torques to the global coordinate system and add them to the generalized force vector.

Detailed geometric data and property data of the leaf spring and suspension system (unsprung mass) is also given in Appendix 1.

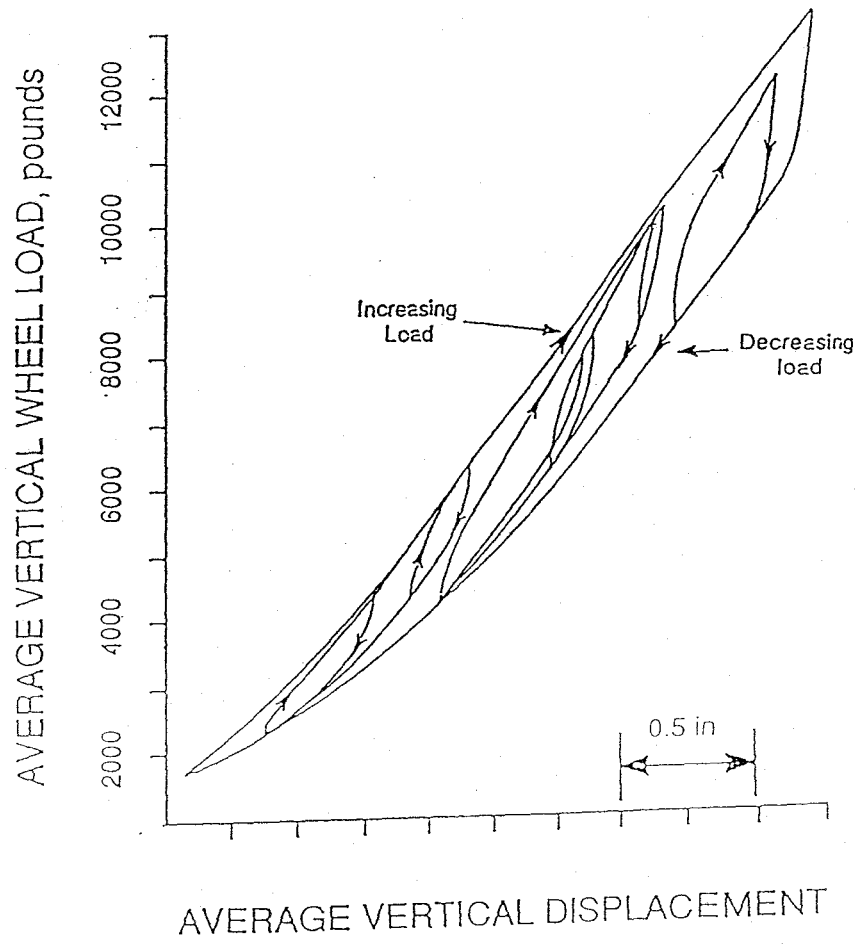


Figure 5
Envelope of Leaf Spring Response

Tire Model

Tires must be considered in any discussion of the vehicle/pavement relationship. The complexity of the pneumatic tire makes it particularly difficult to develop a mathematical model to predict all the tire forces and moments as the general function of the operating condition. However, the initial simplifying assumptions listed below are used in this study;

- 1) Shear stresses in the foot print are negligible, i.e., braking operation is excluded in the pitch/plane motion.
- 2) The tire mass is lumped together with the wheel (unsprung) mass, i.e., the inertia effect of the tire is excluded.
- 3) The pavement is assumed to be rigid.

The vertical and horizontal components of transmitted tire forces is determined by assuming that the tire consists of a linear spring and parallel viscous dampers with facilities for departure from the pavement surface.

Baseline Five Axle Tractor-Semitrailer Model

There are seven bodies (tractor, semitrailer, solid axle, tractor leading tandem axle, tractor trailing tandem axle, semitrailer leading tandem axle, and semitrailer trailing tandem axle) and thirteen degrees of freedom in the two dimensional DADS model of an eighteen wheeler. There are five leaf spring elements and five tire models. Leaf spring elements and tires discussed in the previous sections are modeled as nonlinear force elements.

Simulation Results and Discussion

In order to validate the simulation techniques and to estimate the dynamic wheel load to the pavement, an 18 wheel tractor-semitrailer with leaf spring suspension is simulated on various road profiles at different vehicle speeds. Road roughness and vehicle speed represent two major input variables that are assumed to determine dynamic wheel loading of commercial trucks. Characterization of road roughness is important because excitation of the sprung mass which has a first order effect on dynamic wheel loading, and a road profile having a high wave length that matches the natural frequency of the vehicle at highway designed speed is certainly an undesirable condition. In this study, the effects of joints, and the length of the slab and road profile in the design of parameters in the road surface are considered. The local effects created by the discontinuities are investigated at three different vehicle speeds (30, 45 and 65 mph) with assumption that general road roughness less than 0.1 inch does not directly contribute to the excitation of the sprung mass. Prior to the generation of the nonlinear full vehicle model, a simplified model was used to determine the natural frequencies of the various modes. Table 1 describes the natural modes in the frequency range affecting the tire forces.

Table 1 Vibration Modes of a Tractor/Semitrailer

<u>Mode Description</u>	<u>Frequency (Hz)</u>
Tractor Vertical Translation	2 - 2.8
Semitrailer Vertical Translation	2.6
Tandem Axle Bounce	8.5 - 17

Figure 6 illustrates the difference in dynamic load estimates for the simple and full models for encountering a half inch fault. The load estimates are considerably higher for the more complex representation as shown for even the 30 mph case, indicating that a more complete representation of the vehicle, including the non-linearities, is extremely important if appropriate conclusions are to be drawn from the research.

Dynamic Load Effects of a Slab Fault as a Function of Speed

The step fault excitation theoretically excites all of the vehicle frequencies and provides a simplified method of assessing parameter variation in the vehicle model. For the validation runs, a half inch fault height at a doweled joint on an otherwise flat road profile has been assumed. Two different vehicle speeds (30 mph and 65 mph) are assumed. A typical output, showing the normalized dynamic wheel load for the steer axle at 65 mph is represented in Figure 7. The steer axle hits the fault at the 0.65 second mark indicated by the variation from the steady state equilibrium of the vehicle. There are high peaks around 1.5 seconds and at 1.75 seconds. These responses are matched with the large pitch angle variation of the tractor at about the same time as shown in Figure 8. The two large angle deviations result from the coupling effect of all the dynamic loads and the semitrailer pitch motion. Figures 9 and 10 present the normalized dynamic wheel loads for the tandem axle of the tractor. A slight time lag at the fault shown in the figures matches with the distance between the steer axle and tandem axle set of the tractor. The natural bounce frequency of the tandem axle set is approximately 9 Hz at the observant transient response time of between 3 and 4 seconds. Also, the natural bounce frequency of the tractor estimated from the coupled vibration mode between tandem axle and tractor is approximately 3 Hz. Figures 11 and 12 show the normalized dynamic wheel loads of the tandem axle set of the semitrailer. The initial smooth up and down response is due to the coupled influence of the pitch angle variation of the tractor as shown in Figure 8. Analysis revealed that the small mass of the tractor relative to the loaded semitrailer results in little coupling effect from the tractor to the semitrailer. In contrast, the semitrailer response does tend to affect the tandem axle loading and consequent response of the tractor. The frequencies of the tandem axle bounce and semitrailer bounce are approximately 9 Hz and 3 Hz respectively, the same as for the tandem axle of the tractor.

The previously referred to figures indicate dynamic loads levels about 10% to 20% higher for 65 mph than for 30 mph.

Dynamic Load Effects of Continuous Slab Warping

Although the output of the vehicle model permits detailed analysis by axle as done for the slab fault, a more aggregate measure can make it easier to display the sensitivity of dynamic

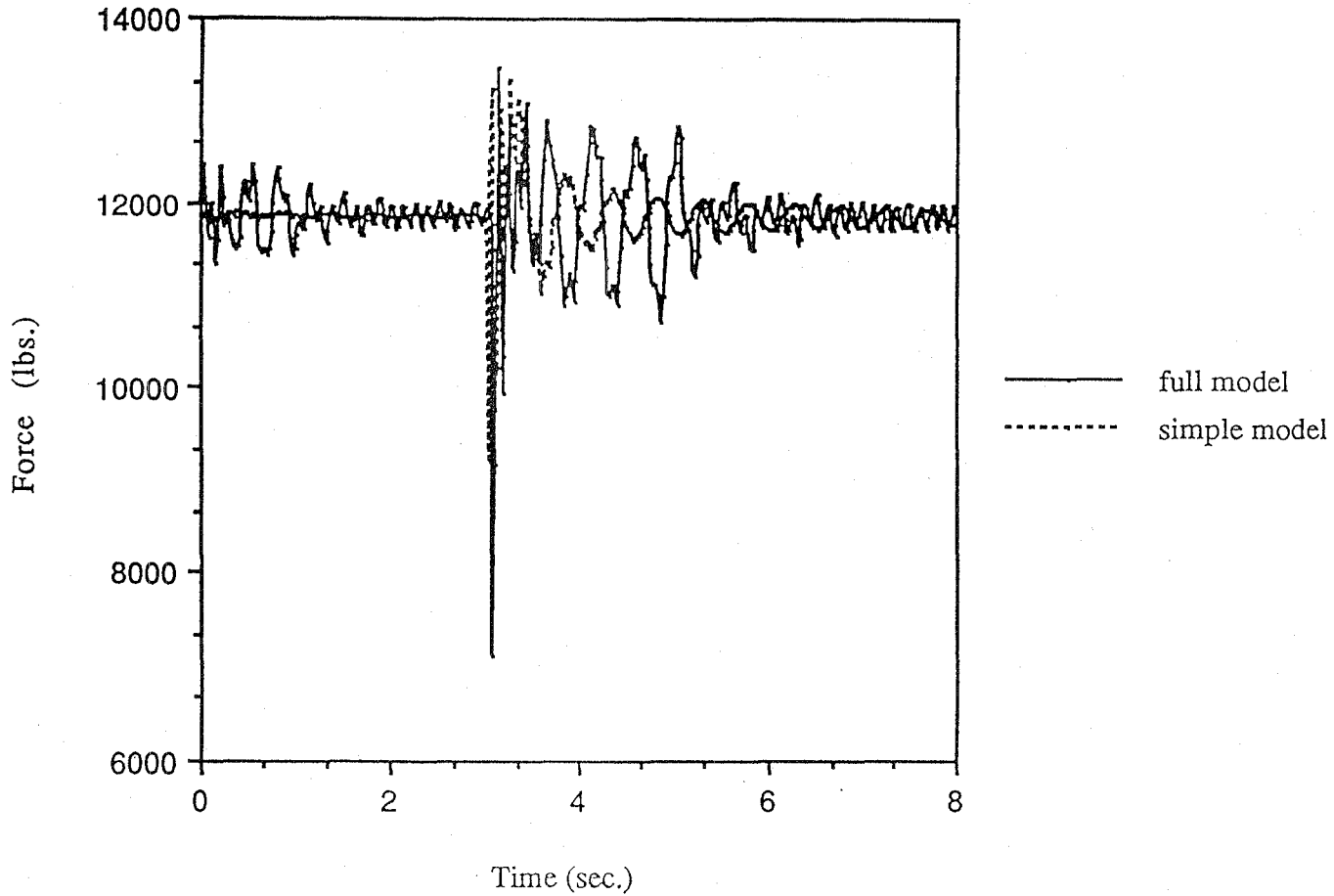


Figure 6
Comparison of Full and Simple Simulation Model Dynamic Load Estimates for Front Axle Hitting a Bump at 30 mph

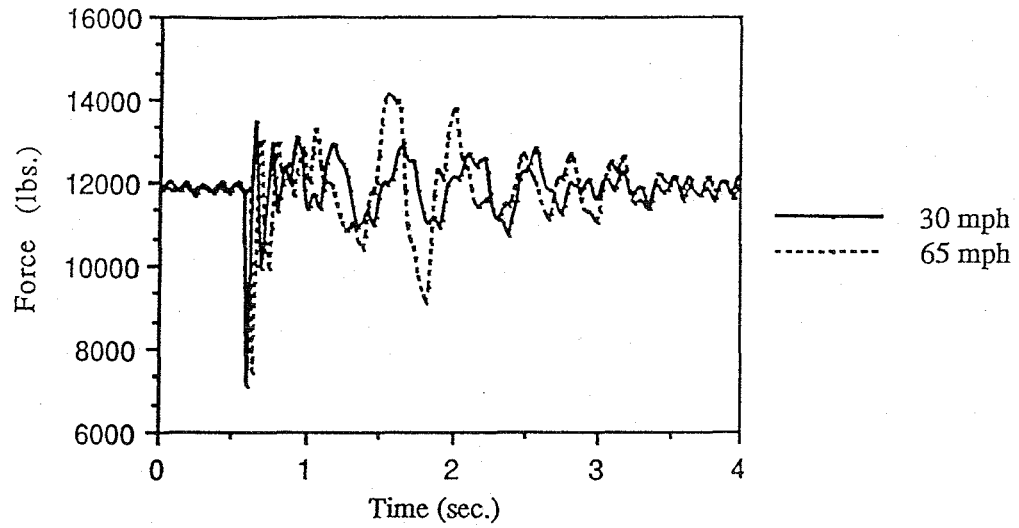


Figure 7
Dynamic Load for the Steering Axle (half inch faulting)

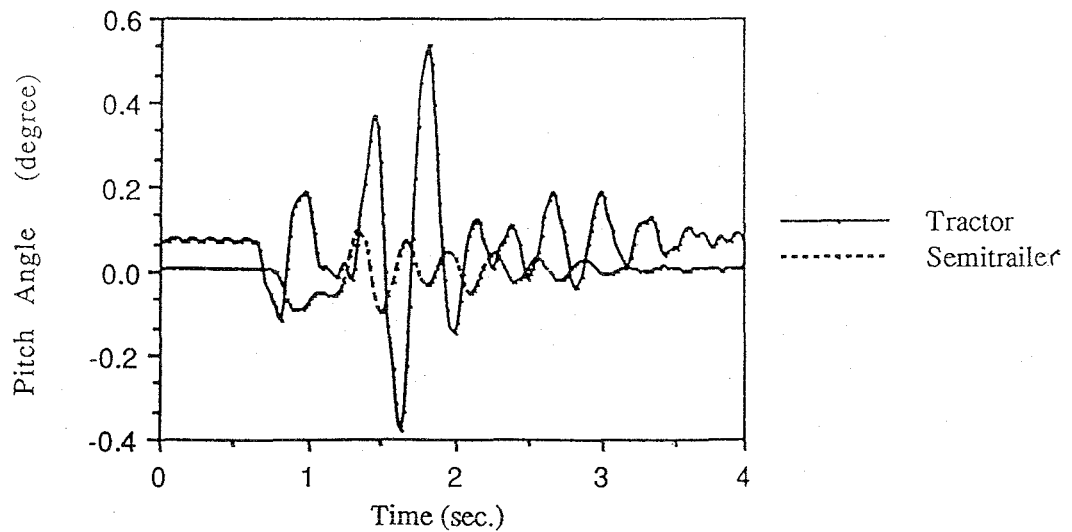


Figure 8
Pitch Angle of Tractor and Semitrailer (half inch faulting and 65 mph)

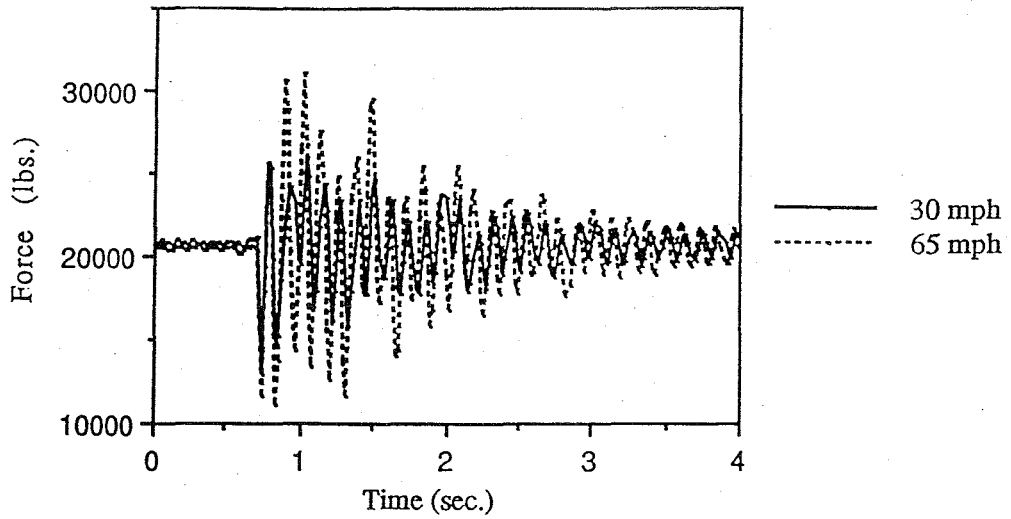


Figure 9
Dynamic Load for the Leading Axle of Tractor Tandem
(half inch faulting)

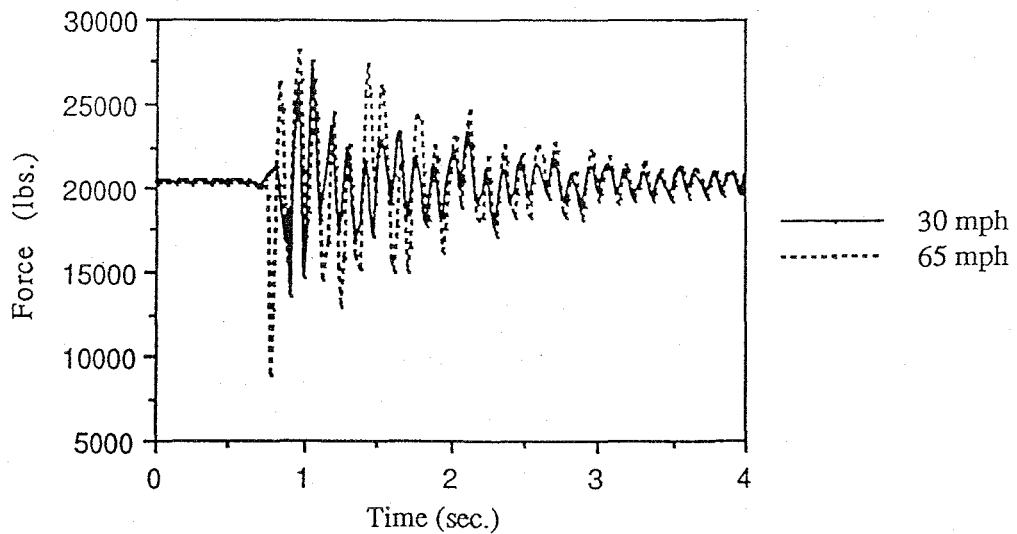


Figure 10
Dynamic Load for the Trailing Axle of Tractor Tandem
(half inch faulting)

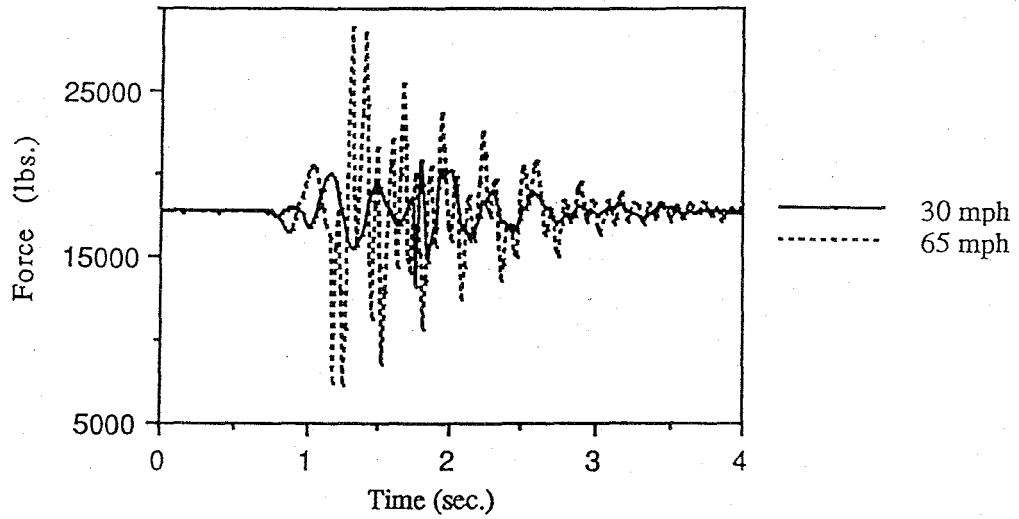


Figure 11
Dynamic Load for the Leading Axle of Trailer Tandem
(half inch faulting)

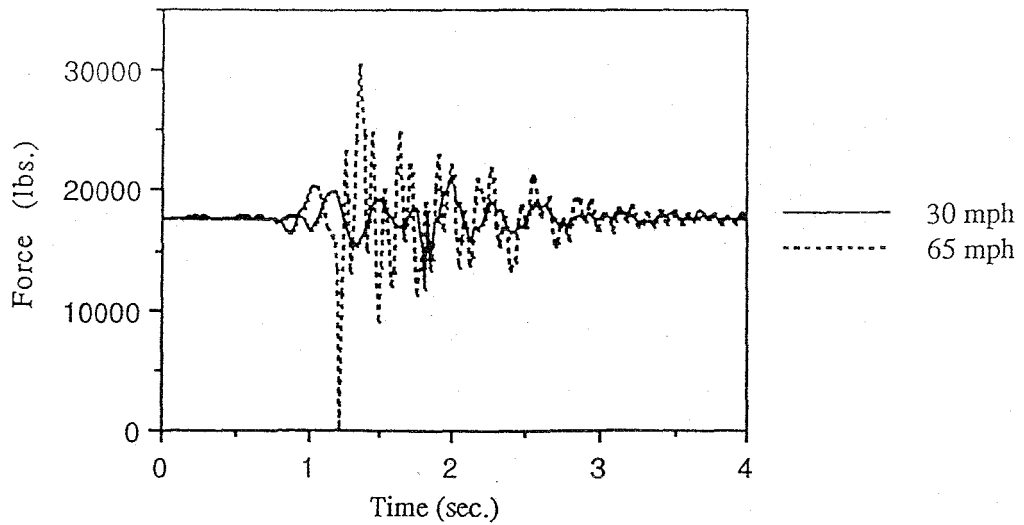


Figure 12
Dynamic Load for the Trailing Axle of Trailer Tandem
(half inch faulting)

loading to pavement and vehicle parameters. The theoretical accumulated axle load response has been used in previous research [2-4]. The procedure adopted in this study was to divide the pavement surface along each wheel path into a number of equal segments. The segment size should be sufficiently small to enable resolution of the peak forces up to the highest frequencies of the interest. The mean aggregate load is determined by averaging the aggregate load over several slabs to suppress any transient dynamic effects. The mean aggregated load is then normalized by the vehicle static load. The periodic slab warping corresponds to an input to the vehicle of 2.2 Hz for 30 mph, 3.3 Hz for 45 mph, and 4.8 Hz for 65 mph. Figure 13 shows normalized aggregate load along the slab which is, as expected, for there is a periodic wheel load response that coincides with the slab length. The heaviest loading is sustained in the edge of the slab due to the excitation of the lower frequency body mode. For all three speeds, dynamic load in the latter part of the slab (where the vehicle leaves the slab) is higher than for the front (where the vehicle enters the slab). This could be a factor in creating the eventual resulting faulting condition. When the vehicle speed is 30 mph, 45 mph, or 65 mph, the respective highest peak point is about 5%, 23%, and 15% above the static load. The case for 45 mph is the highest among three cases. This can be explained by noting that the frequency for 45 mph coincides with the natural bounce frequency of the tractor and semitrailer, a factor that significantly influences the changes in dynamic loading conditions observed in Figure 13. As a result, it can be expected that the frequency at which the vehicle experiences these inputs should be adjusted so that it is not in the range of the body mode frequency. The adjustment could be made by either regulating vehicle speed or changing the design slab length.

It is important to understand that the aggregated force at a point depends upon the cumulative effect of all vehicle axles that pass over it. Therefore, the maximum aggregate forces will not necessarily occur at the same location as the maximum force generated by any individual wheel. Figure 14 shows an example for 30 mph case (maximum aggregate load occurs in the three quarter region of the slab). Maximum loads for the steer axle (curve 1) occurs at the middle of the slab, and those of tandem axles of tractor (curves 2 and 3) occur in the two-thirds region of the slab.

Figures 15 and 16 show the maximum forces for the 45 and 65 mph cases respectively. Note that the 45 mph case produces the highest dynamic loads from the trailer tandem and that the peak impact loads occur near the 20 foot joint locations.

Effect of velocity on the real road profile

Weigh-in-motion (WIM) technology has been applied to both the gathering of background data for size and weight enforcement and the generation of axle weight distributions for design and planning. In-motion-weighing of a highway vehicle approximates the weight of a vehicle, a wheel, an axle, or a group of axles, by measuring the vehicle component of the total dynamic force applied to the pavement surface by successive tires. In order to compare with the results from WIM calibration, the vehicle was simulated on the same geometric road profile as the road where WIM test sites are located on a section of interstate highway 80. Figure 17 shows a section of real road profile and location of WIM test site. Figure 18 shows the aggregated dynamic wheel load for two different vehicle speeds: 30 mph and 65 mph. the aggregated dynamic load for both cases at the WIM site is within 5% of the total static load.

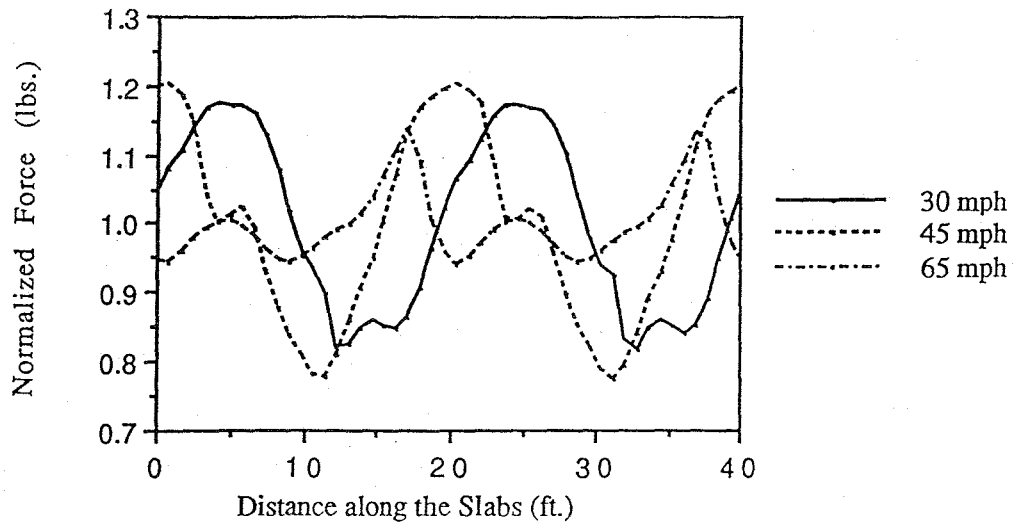


Figure 13
Aggregate Dynamic Load for Continuous Slab Warping
(20 ft. slab length)

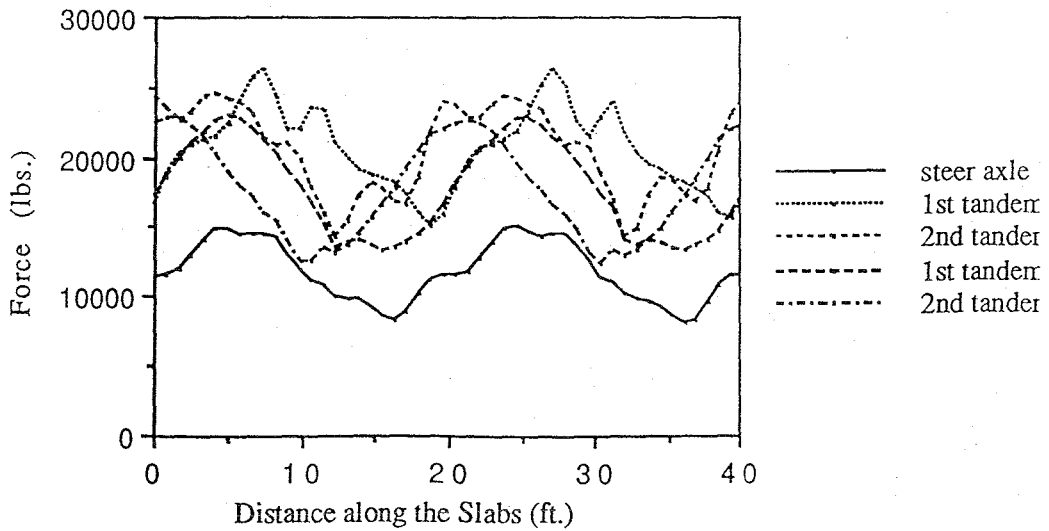


Figure 14
Dynamic Wheel Loads for each Axle for Continuous Slab
Warping (30 mph and 20 ft. slab length)

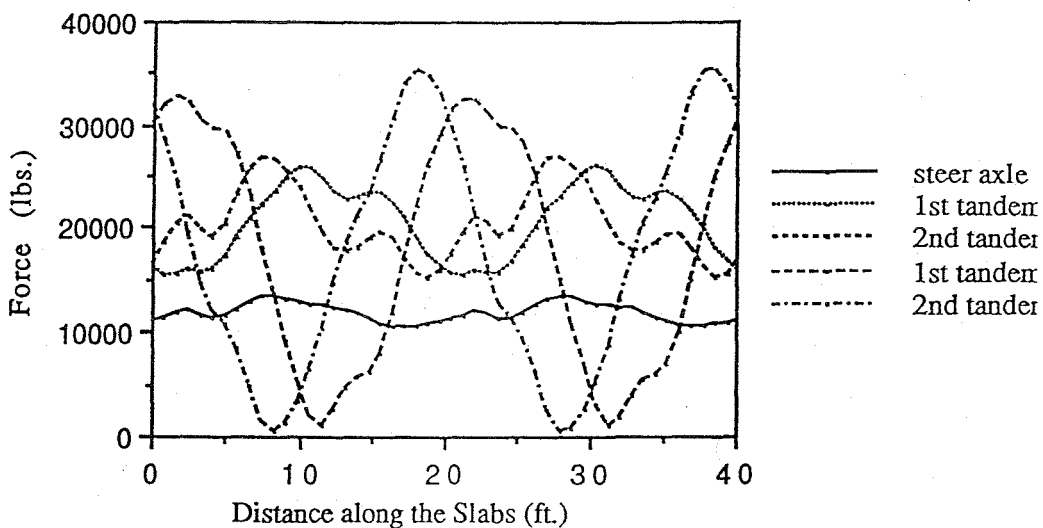


Figure 15
Dynamic Wheel Load for Each Axle for Continuous Slab
Warping (45 mph and 20 ft slab)

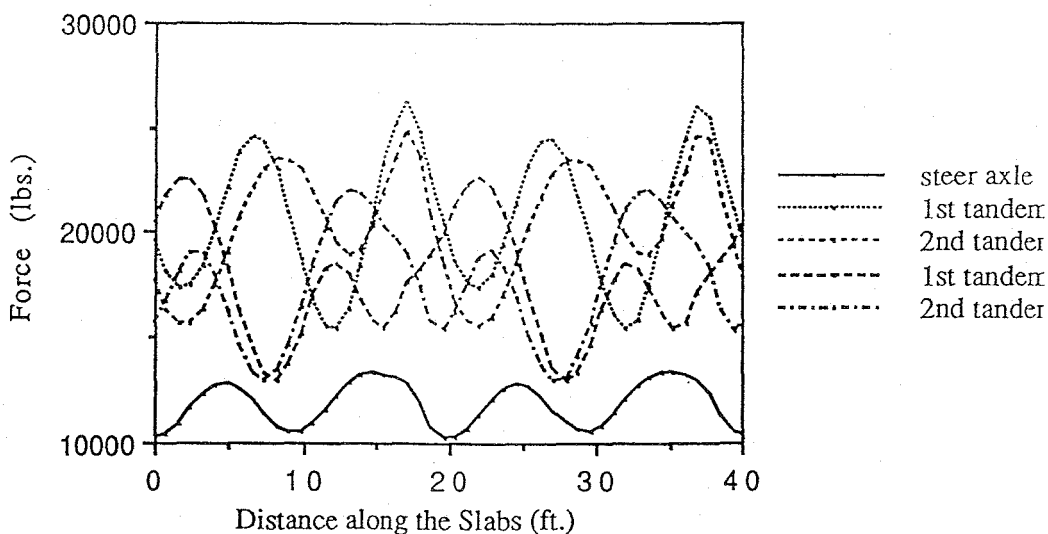


Figure 16
Dynamic Wheel Loads for Each Axle for Continuous Slab
Warping (65 mph and 20 ft slab)

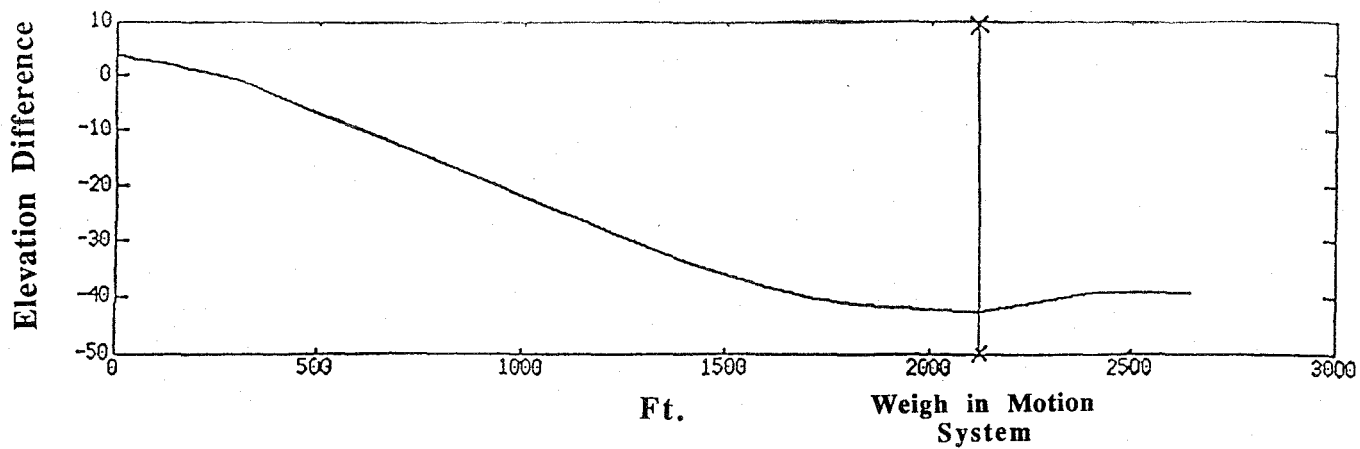


Figure 17
Approach Profile for Instrumented Test Segment

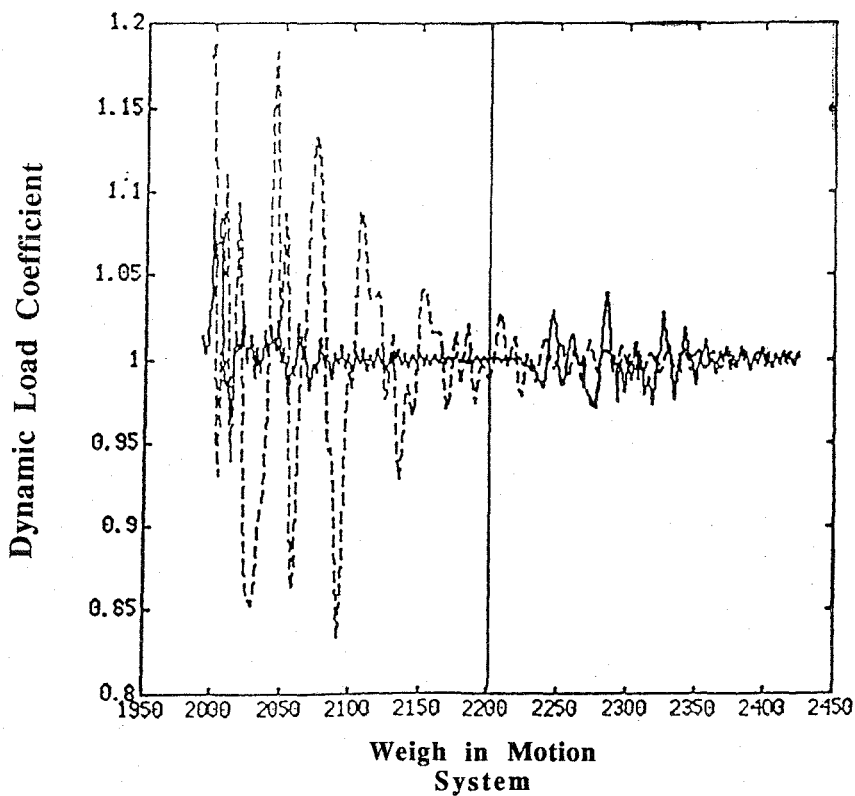


Figure 18
Aggregate Dynamic Load Coefficient for Instrumented Test Pavement at 30 and 65 mph

Three-Dimensional Model

The previously described two-dimensional tractor-trailer model allowed for only three degrees of freedom for each body before the inclusion of constraints, namely longitudinal and vertical translation, and pitch. A three-dimensional model would add another three degrees of freedom for each body: lateral translation, roll, and yaw. While the two-dimensional vehicle model is sufficient for most studies, it becomes necessary to utilize a three-dimensional vehicle model to capture certain effects. From the vehicle dynamics standpoint, some important issues that the two-dimensional model cannot accommodate are:

- 1) **Vehicle handling.** It is known that semi trailers exhibit yaw instability even without steering input. Therefore the yaw degree of freedom must be included in the model in order to investigate yaw instability.
- 2) **Cornering.** The lateral translational and yaw degrees of freedom must be included in any model that is to be used to study the effect of steering on the vehicle behavior. Also, if vehicle rollover during cornering is of concern, then the roll degree of freedom must be included in the vehicle model as well. The roll degree of freedom also contributes to the steering behavior through the roll steer effect.
- 3) **Unsymmetrical road input.** This situation could occur with skewed joints in the pavement, for example. In any event, the roll degree of freedom must be included in the vehicle model in order to account for differing heights of the road surface between the left and right sides of the vehicle.

Of course, it is possible to investigate these phenomena with specialized models, such as a yaw-plane model for studying the cornering behavior of the vehicle. However, the interaction among the degrees of freedom would not be accounted for. It may be more convenient to have only one vehicle model that can be used to study motion in any of the possible degrees of freedom, rather than having several specialized models that are tailored for investigating only one particular aspect of vehicle behavior.

From the pavement response standpoint, the three-dimensional vehicle model is needed in order to supply the differing tire forces that are due to skewed joints or unsymmetric pavement heights to the finite element model, since the differing left and right side tire forces will produce unsymmetric pavement deflections.

Major Differences in Modeling

The commercial DADS software was used to simulate maneuvers with the two-dimensional vehicle model. However, with the increase in dimension of the system of equations that accompanies the increase in the number of degrees of freedom in the three-dimensional model over the two-dimensional model, the amount of Central Processing Unit time required for the completion of a simulation may become too long to be tractable. Therefore, it is desired to utilize the relative coordinate dynamics formulation for simulating maneuvers with the three-dimensional model [7].

The modeling of the steering system is not trivial. Steering systems have complicated kinematics, with nonlinear bushings used as connections for many, if not all, of the joints between the individual components. The compliance of the steering system is an important effect; however, it is possible to approximate the behavior of the steering system with rigid joints. This simplification has the additional advantage of avoiding the introduction of mathematical stiffness into the system of equations due to the physical stiffness of the bushings when they are modeled as force elements.

Animation

The simulation of dynamic systems produces position, velocity, acceleration, and force information. However, this information becomes difficult to interpret for most mechanical systems due to the large number of elements that can be in motion. The possibility of animating the motion of a mechanical system is a valuable tool in interpreting the time history of position information.

FINITE ELEMENT ANALYSIS OF RIGID PAVEMENTS

Modeling Procedures

The most common way of approaching the analysis of rigid pavements is through the use of a two-dimensional plate bending model which is supported on a representation of the subgrade.

Subgrade representation

There are two ways of representing the subgrade conditions; either assuming the subgrade as a liquid foundation, also known as a Winkler foundation, or assuming the subgrade as an elastic half space. The Winkler subgrade is unable to transfer shear stresses. This means that the reaction at any point of the base (vertical pressure) is proportional only to the deflection of the slab at that point. This is different from the elastic solid representation of the foundation, in which the subgrade is capable of transferring shear stresses. In the later case, the reaction at a point at the base depends not only on the deflection of the slab at that point, but also on the deflection of adjacent points. Figure 19 illustrates the two representations of the subgrade.

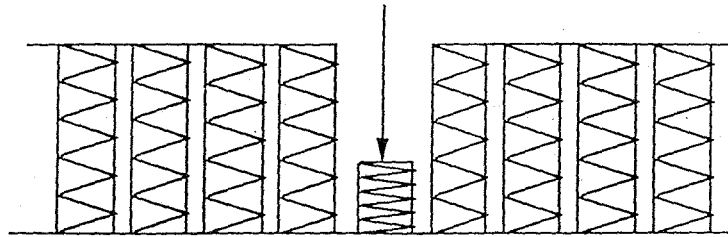
It is assumed for this work that the subgrade behaves as a Winkler foundation. The constant of proportionality between the slab deflection and the reaction is known as the modulus of subgrade reaction, k . It is defined as the pressure necessary to produce a unit deformation of the subgrade and is determined through plate loading tests at a standard plate radius of 15 inches (Ullidtz, 1987).

Pavement representation using ANSYS

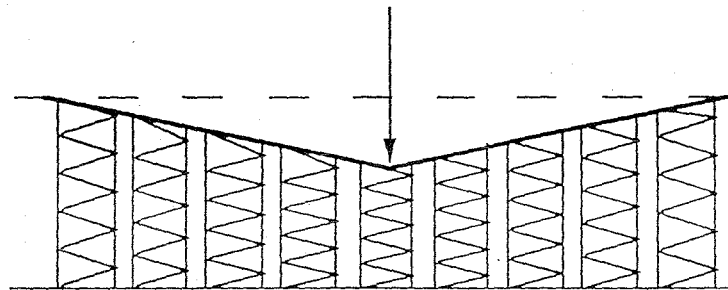
ANSYS, a general purpose finite element program, is selected for analysis of rigid pavements. The slab is represented by plate elements and the foundation by a series of vertical springs located at different nodes. Two different elements are available in the ANSYS element library that are suitable for pavement modeling. They are identified as STIF63 and STIF91.

STIF91 is defined geometrically by eight nodes and can accommodate layers of different material properties through the pavement thickness. This capability allows for a realistic representation of pavements on stabilized subgrades. Figure 20 presents the geometrical configuration of this element as well as the input and output information. The springs representing the subgrade reaction are located at each node. They have a stiffness constant equal to the modulus of subgrade reaction (k) times the influence area surrounding the node. Figure 21 shows the location of these springs in a tentative mesh, as well as the area of influence of each one.

STIF63 is a four-node quadrilateral plate element supported on Winkler foundation. This element assumes only one layer through the pavement thickness. It is a convenient element to use because it does not require separate input for the springs representing the foundation. Internally this element is formed from a condensation of four triangular thin plate elements and is known to be a relatively *stiff* element. The deflections obtained with STIF63 are on the average, 3% smaller than those obtained with STIF91.



a.) Winkler Foundation.



b.) Elastic Solid Foundation.

Figure 19
Representation of Winkler and Elastic Subgrades

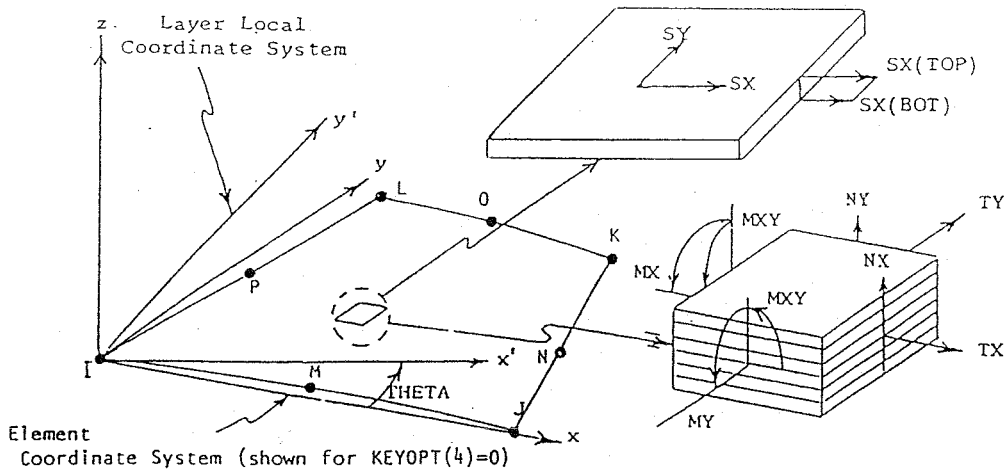
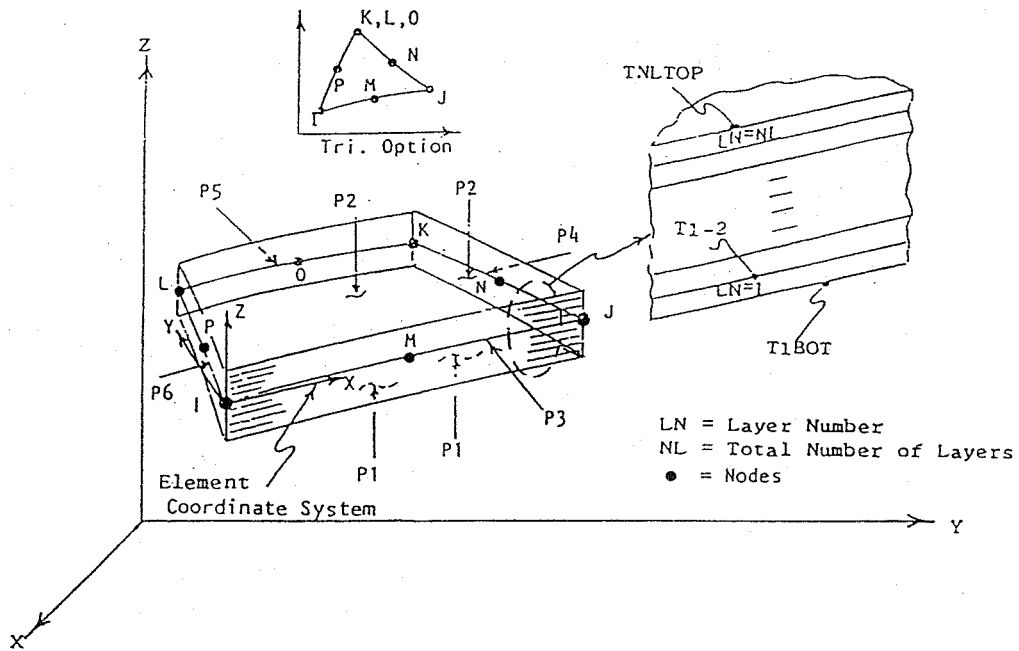


Figure 20
 ANSYS/STIF91 Eight Node Layered Shell

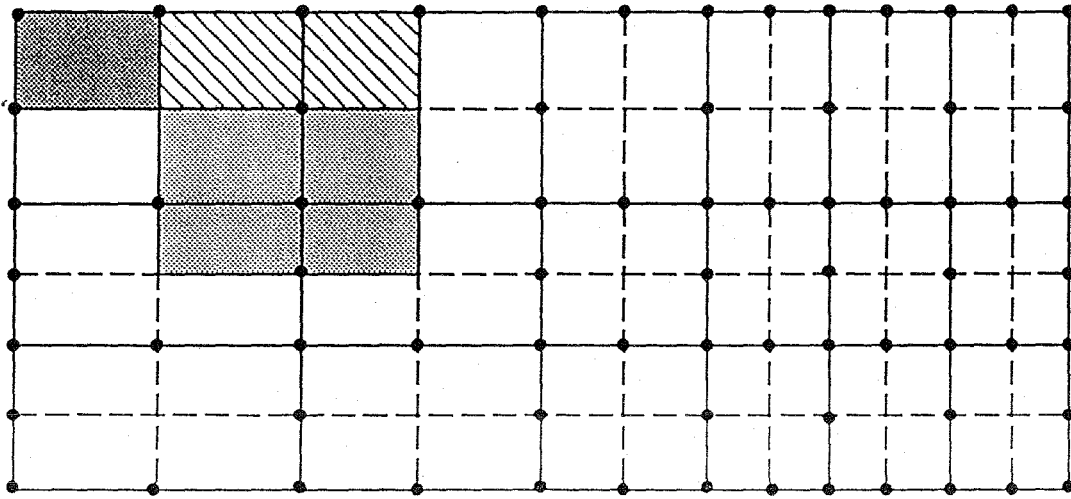


Figure 21
Springs Location for STIF91 and Influence Areas

Validation of Model

In order to test the model described above, a series of pavements presented in the work by Chou (1981) were modeled and the results compared with those given by the finite element program WESLIQID (Chou, 1981).

Example 1

The pavement geometry, load location and material properties are presented in Figure 22. In order to facilitate comparison of results, the same mesh was used in ANSYS as was used in WELIQID. Since the pavement had only one layer, element STIF63 was used.

The results from the ANSYS model compared well with those reported by Chou (1981). The maximum difference between the deflections obtained by Chou and those obtained by ANSYS is 1.4% .

Example 2

This example is used to check the results against the ones provided by the Westergaard's solution. The test pavement is rectangular, of sides measuring 20L and 10L, with L being the radius of relative stiffness of the slab and subgrade. It is given by:

$$L = \left[\frac{E t^3}{12 (1 - n^2) k} \right]^{.25}$$

E = Young's modulus of the pavement.

t = thickness of the pavement.

n = Poisson's ratio of the pavement.

k = modulus of subgrade reaction.

A concentrated load is applied on one edge. Figure 23 presents the mesh layout used in the analysis; owing to symmetry only half of the structure was modeled. Figure 24 presents the graph provided by Chou (1981) showing the Westergaard's solution. The STIF63 element was used for this analysis.

The results obtained using ANSYS differ between 5% and 10%, primarily due to distortion in estimating the values from the graph.

Example 3

The third example is presented in Figure 25, along with the material properties. The example consists of two pavements connected by dowel bars. The pavement is represented by STIF63 of ANSYS. The dowel bars are represented by a three dimensional beam element located at the corner nodes of the plate elements. The length of the bar elements equals the gap between the slabs.

The results obtained in this case are in general about 20 to 25% less than those reported by Chou(1981). This is a large difference, but one constant throughout the slab. It is believed that the reason for this discrepancy is the existence of a stabilized sub-base. The reference did not report the characteristics of the stabilized sub-base.

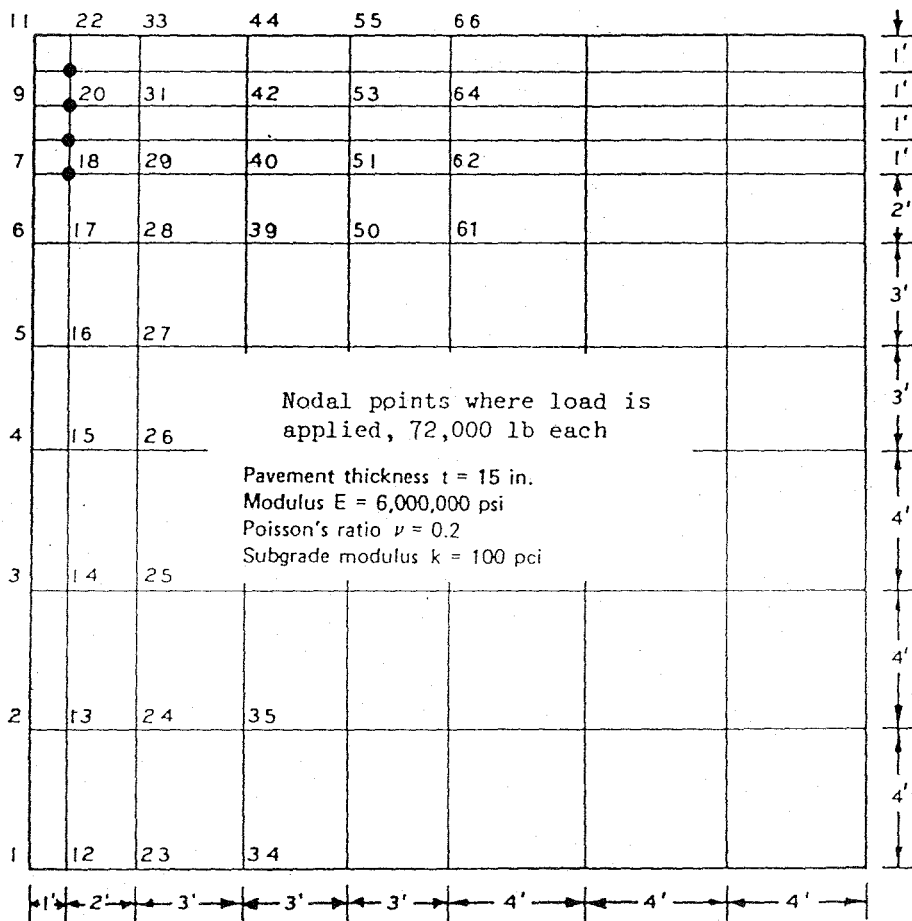


Figure 22
 Mesh Layout and Material Properties for Example 1. Chou
 (1981)

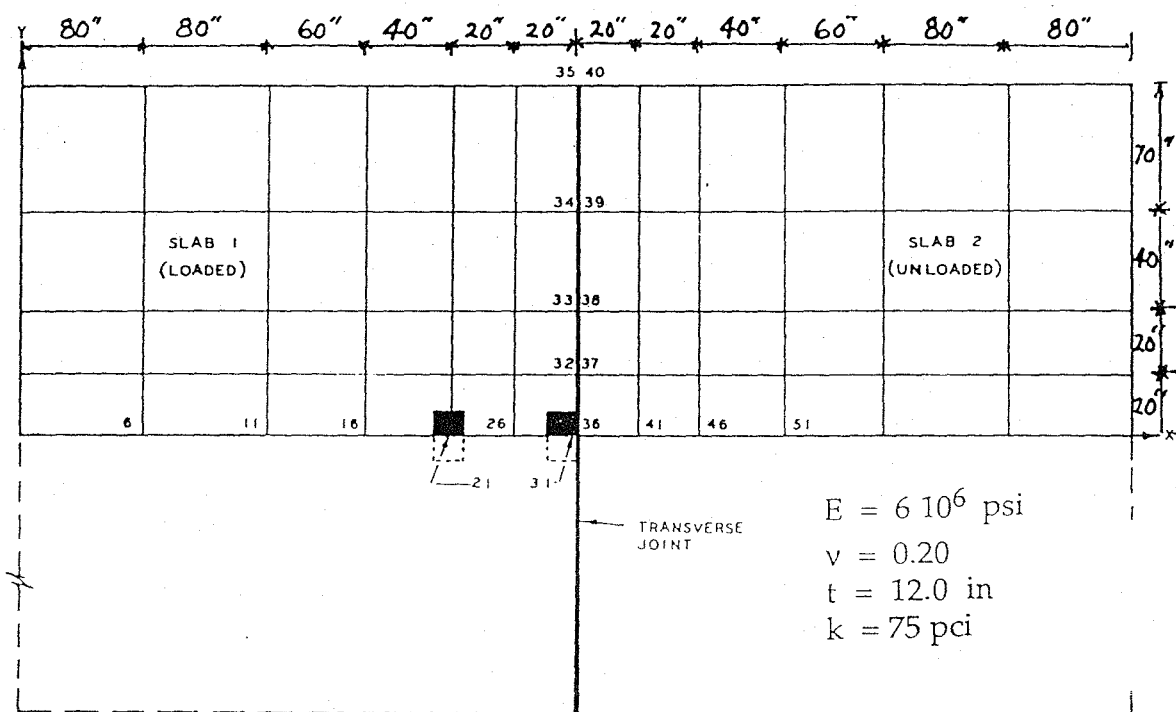


Figure 23
Mesh Layout Used by Chou (1981)

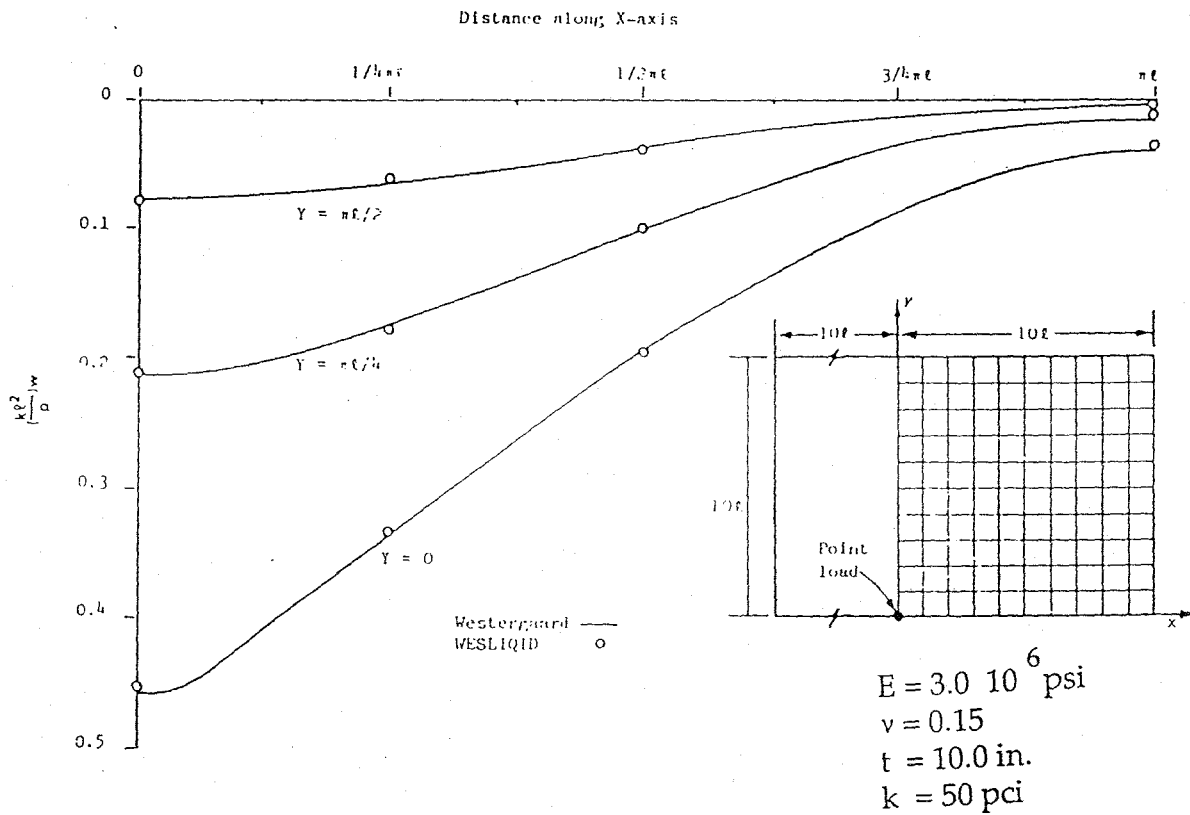


Figure 24
 Comparison of WESLIQID Finite Solution with Westergaard's
 Solution, deflections (Chou, 1981)

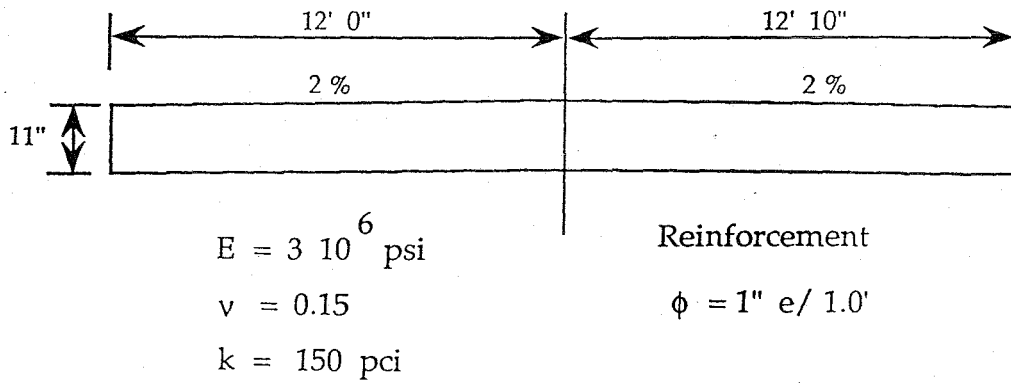


Figure 25
Slab Cross Section with Material Characteristics

Pavement Response Analysis Procedure

The task of computing pavement response to a moving vehicle load is divided into two parts.

1. Estimation of dynamic forces at tire-pavement contact points

The first task is to estimate the dynamic forces at tire-pavement contact points. Forces are estimated by simulation of a vehicle with known characteristics traveling over a pavement with known or assumed imperfections. The work is performed by the Dynamic Simulation group using DADS software, and is documented in the earlier section of this report. For the purpose of this simulation the pavement is assumed rigid. Thus the interaction between the pavement response and the vehicle is neglected. The end result of dynamic simulation is a set of dynamic forces as functions of time at tire pavement contact points.

2. Pavement response calculations

Once the tire contact force histories are known, the pavement response calculations phase begins. Here it is important to devise an efficient solution strategy because of a need to analyze several different vehicle and pavement characteristics. A straight forward way of computing dynamic pavement response is to use the dynamic analysis capabilities of the computer program ANSYS and directly obtain time histories of pavement response. However this procedure is not very efficient because it will require a complete dynamic finite element analysis for each different simulation. A more efficient procedure is employed, based on influence lines and the principle of superposition. Different steps involved in the procedure are explained in the following paragraphs.

Generation of influence curves

An influence curve for a particular point on the pavement represents response (pavement deflection in this case) at that point as a unit load travels along a wheel path. To construct an influence curve, we must first select a traveling path (a line along which the vehicle is assumed to move) given by line 2-7-12-17-22 in Figure 26. In the discretized finite element model a unit load is placed successively at each node along this path and deflection response at the reference point is computed and saved resulting in an influence curve. This procedure can also be applied to construct more than one influence curve simultaneously. For this purpose, many load sets as points are defined along the traveling path. For each load set, the unit load is placed at a different node path in consecutive order. Referring to Figure 26, the load set 1 will consist of the unit load applied at node 2; load set 2, of the unit load applied at node 7; load set 3, of the unit load applied at node 12; etc. For a load set i , the nodal deflection values δ_j^i ; $j = 1, \dots, n$; where n is the number of nodes along the traveling path), are saved. Thus δ_j^i represents deflection δ at node j when the unit load is applied at node i . These response values are saved in a two dimensional array $RESP_d(n, n)$. After all the load steps are completed, this array will have a distribution similar to that shown in Figure 27. Each row of this array represents an influence curve for a node number that corresponds to the row number in the array.

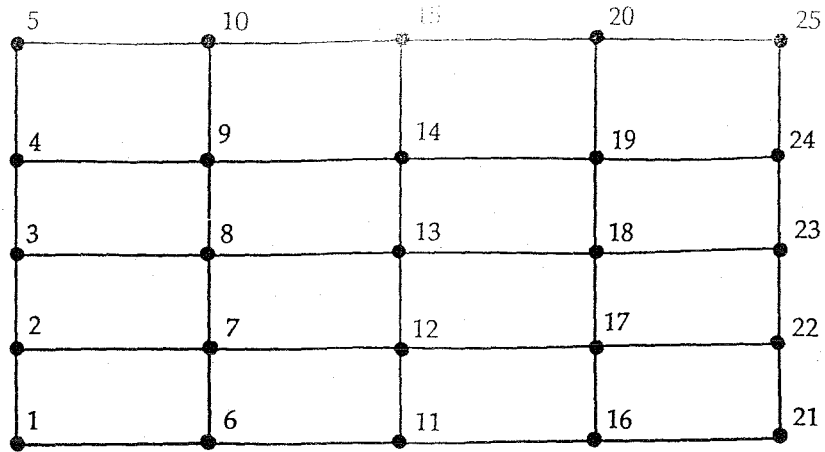


Figure 26
Nodal Array to Finite Model

	Load set 1	Load set 2	Load set 3	Load set 4	Load set 5
#2	δ_2^2	δ_2^7	δ_2^{12}	δ_2^{17}	δ_2^{22}
#7	δ_7^2	δ_7^7	δ_7^{12}	δ_7^{17}	δ_7^{22}
#12	δ_{17}^2	δ_{12}^7	δ_{12}^{12}	δ_{12}^{17}	δ_{12}^{22}
#17	δ_{12}^2	δ_{17}^7	δ_{17}^{12}	δ_{17}^{17}	δ_{17}^{22}
#22	δ_{22}^2	δ_{22}^7	δ_{22}^{12}	δ_{22}^{17}	δ_{22}^{22}

Figure 27
Nodal Response Matrix

Response curve for a particular node

A response curve for a point shows the response (deflections in this case) as a vehicle travels over a segment of the pavement. Dynamic forces for each axle are known as a function of time from the vehicle simulation. Knowing the speed of the vehicle (assumed to remain constant during simulation) these forces can be easily converted into force versus distance along the pavement.

The response at a point due to a single axle can be computed by multiplying the ordinate of the influence curve at that particular point with the force at that point from the force versus distance profile. For multiple axles, the response curve are first generated separately. Then, a superposition of these provides the response curve due to all vehicle axles. During this superposition the individual axle responses are shifted by distances equal to the distance between the axles. The steering axle is taken as reference. Each response curve for the remaining axles is shifted, in the direction of travel, by the distance between the steering axle and the axle under consideration.

The final response curve for a particular node represents the total response at that node as the vehicle moves along the wheel path with the position of the vehicle characterized by the position of the steering axle.

Vehicle and Pavement Models for Parametric Studies

A five axle tractor-trailer, with geometric characteristics shown in Figure 3, is used as the base vehicle for this parametric study. The data needed for dynamic simulation, such as mass distribution and suspension characteristics were selected to be typical such production vehicles. Details of the dynamic simulation are presented in the second section of the report.

The pavement for parametric study consists of eight 20 ft long and 24' 10" wide segments. Only the two middle segments (called test segments) are monitored for analysis results. Three segments before and three after the middle two segments provide continuity of the pavement. The complete finite element model, material characteristics, and slab cross section are shown in Figure 28. The pavement characteristics are similar to those of the Iowa DOT test site on I-80 near Avoca, Iowa.

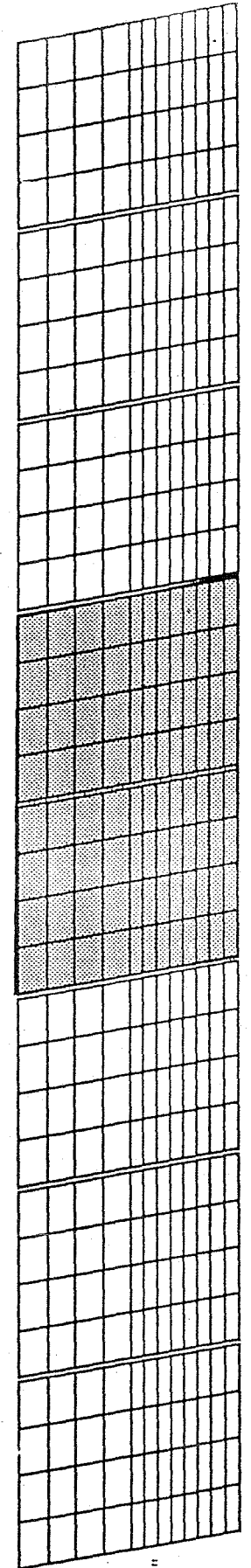
Results of the Parametric Studies

In this phase of the study a planar vehicle model is used to study the effect of different vehicle speeds and pavement roughness characteristics on the deflection response of the pavement. Numerical results are included for the following cases

(i) 1/2 inch bump in the pavement at the start of the test segments with two different vehicle speeds, 30 mph and 65 mph.

(ii) 1/2 inch fault in the pavement at the start of the test segments with two different vehicle speed, 30 mph and 65 mph.

(iii) 1/4 inch continuous faulting in the pavement ("saw-tooth" arrangement) with three different vehicle speeds, 30 mph, 45 mph, and 65 mph.



24' 10"

20' 00"

Figure 28
Pavement Model for Parametric Study

(iv) 1/4 inch continuous warping in each pavement segment with three different vehicle speeds, 30 mph, 45 mph, and 65 mph.

(v) I-80 pavement profile at the Iowa DOT test site with 30 mph and 65 mph vehicle speeds.

All of the above cases assume that the vehicle is loaded with full capacity pay load. The continuous warping case with 45 mph vehicle speed is repeated again without any pay load (empty vehicle). Pavement deflection envelopes for two additional cases are also presented in which constant axle forces approximately equal to static axle loads for full and empty vehicles are applied. These serve as reference cases to understand the importance of the dynamic effects in the pavement response.

1. Presentation of response results

For each case listed above plots are provided showing following results

(i) Plots of axle forces as function of distance from the start of the pavement model. Thus the distance axis (x-axis) is labeled from 0 to 160 ft (8 slabs each 20 ft long). Note that the response results are monitored for the middle two slabs only. Thus forces between 60 ft and 100 ft will have the greatest influence on the response.

(ii) The envelopes of maximum deflections (displacements) at nodes along the travel path. These maximums are obtained from the nodal response curves. The x-axis of the envelopes represents distance of a point from the start of the test slab. Thus the range is from 0 to 40 ft. The vertical axis gives the maximum deflection (in inches) at a point as the vehicle travels over the entire segment pavement segment modeled.

2. Results for 1/2 inch bump case

A 1/2 inch bump is assumed in the pavement at the start of the test segment. The dynamic forces at the axles for the two speeds are shown in Figures 29(a)-(e). As might be intuitively expected, the forces for the 65 mph truck speed are larger as compared to those for the 30 mph speed. The maximum displacement envelope is shown in Figure 30, indicating that the slab joints have the largest absolute displacements. The center points of the slabs do not deflect as much. The 65 mph speed produces higher deflection at the start of the test segment but at the junction of the two segments, a 30 mph speed produces slightly larger deflections.

3. Results for 1/2 inch fault case

A 1/2 inch fault is assumed in the pavement at the start of the test segment. The dynamic forces at the axles for the two speeds are shown in Figures 31(a)-(e). Just as in the bump case, the forces for the 65 mph truck speed are greater than those for the 30 mph speed. The frequency content of these dynamic forces is similar to the bump case. The maximum displacement envelope is shown in Figure 32. Again, the envelope shows that the slab joints experience the largest absolute displacements. Contrary to the bump case, the 30 mph speed produces a slightly larger deflection at the start of the test segment, but at the junction of the two segments, the 65 mph speed

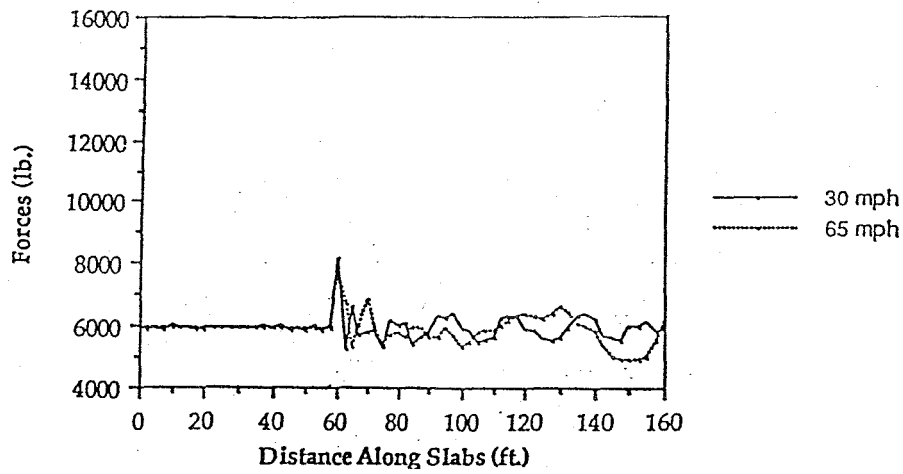


Figure 29 (a)
Dynamic Wheel Path Load for Steering Axle
(half inch bump)

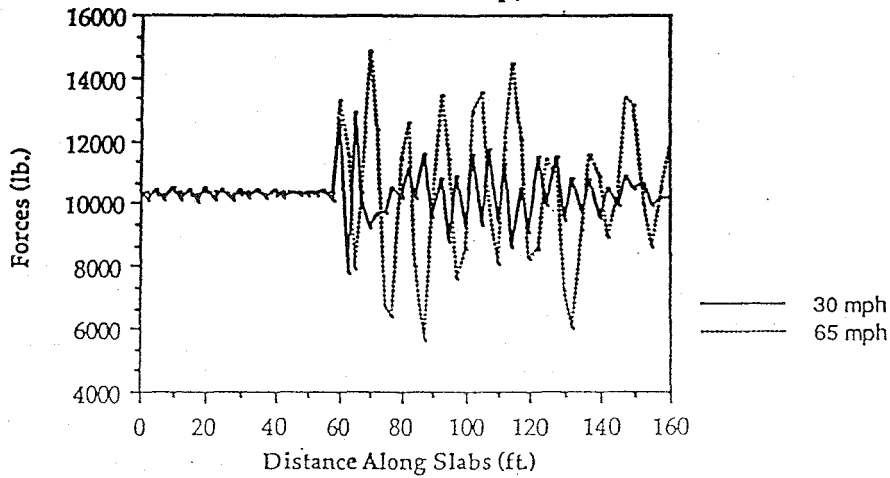


Figure 29 (b)
Dynamic Wheel Path Load for Leading Axle of Tractor Tandem
(half inch bump)

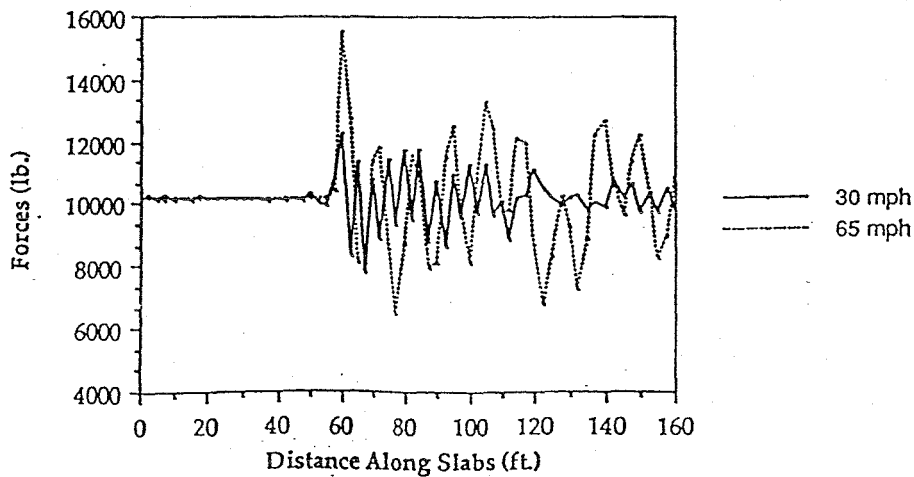


Figure 29 (c)
Dynamic Wheel Path Load for Trailing Axle of Tractor Tandem
(half inch bump)

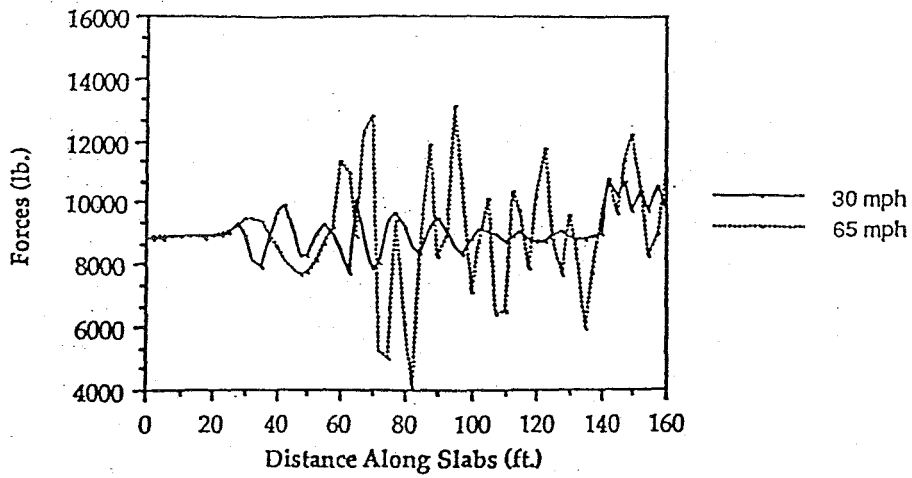


Figure 29 (d)
Dynamic Wheel Path Load for Leading Axle of Semitrailer Tandem
(half inch bump)

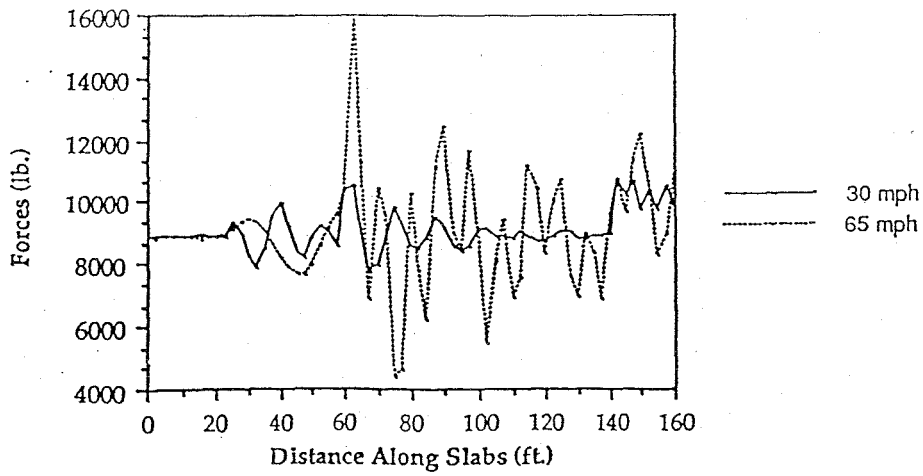


Figure 29 (e)
Dynamic Wheel Path Load for Trailing Axle of Semitrailer Tandem
(half inch bump)

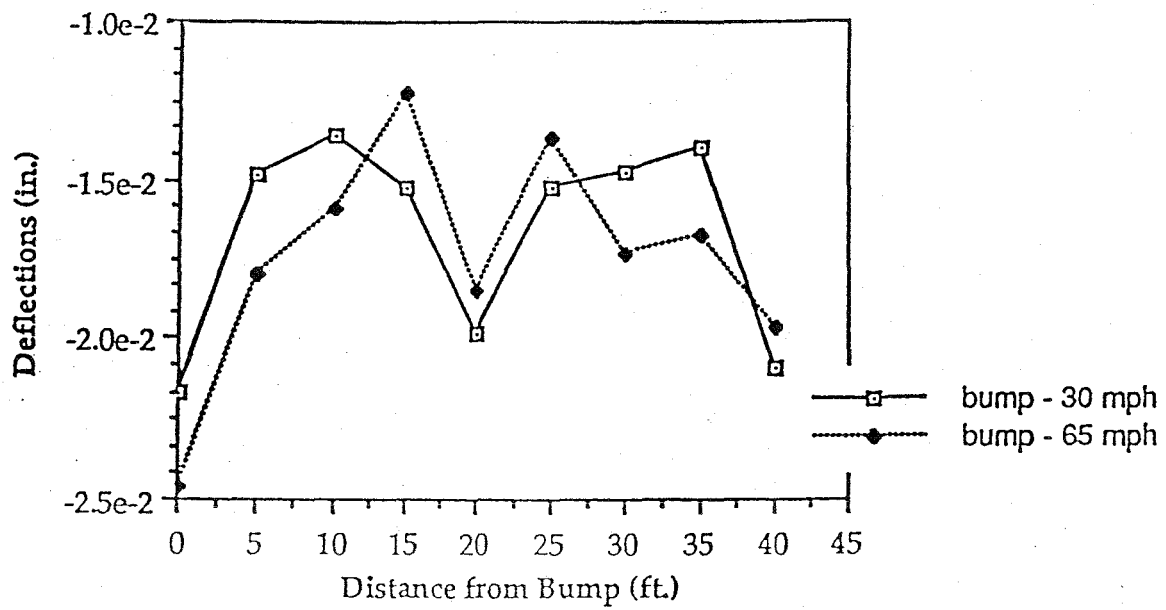


Figure 30
Envelope of Maximum Slab Displacement for Bump Case

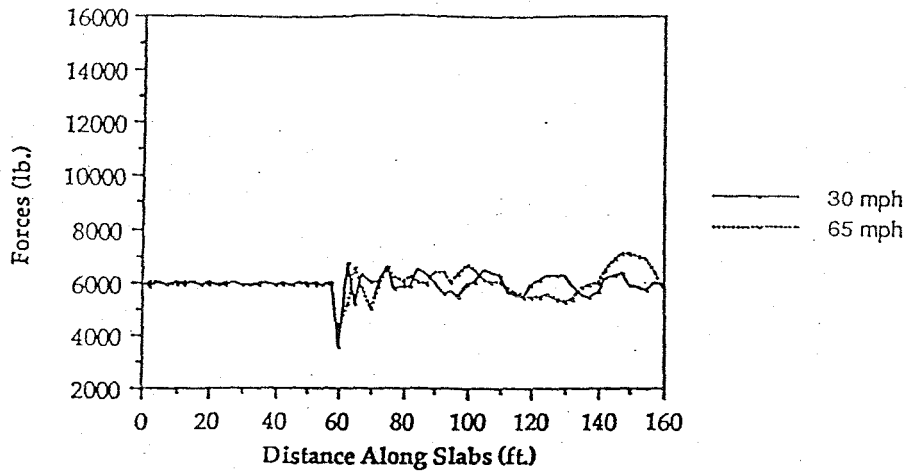


Figure 31 (a)
Dynamic Wheel Path Load for Steering Axle
(half inch fault)

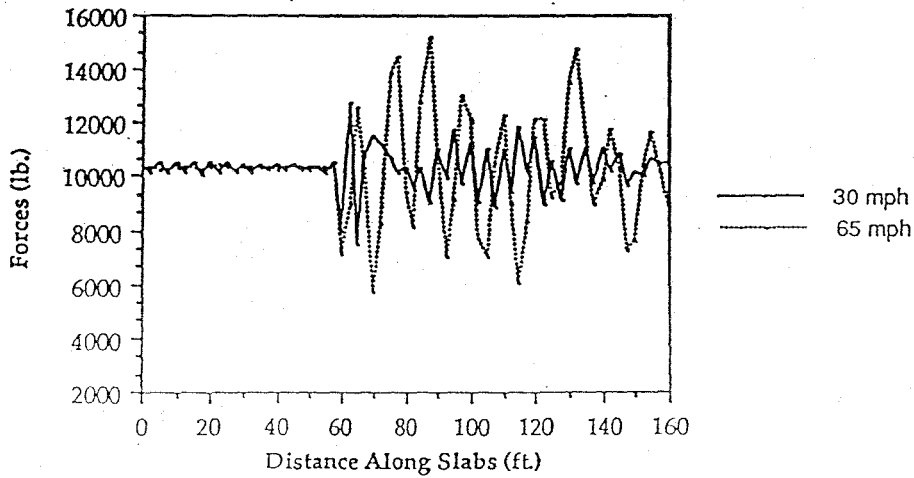


Figure 31 (b)
Dynamic Wheel Path Load for Leading Axle of Tractor Tandem
(half inch fault)

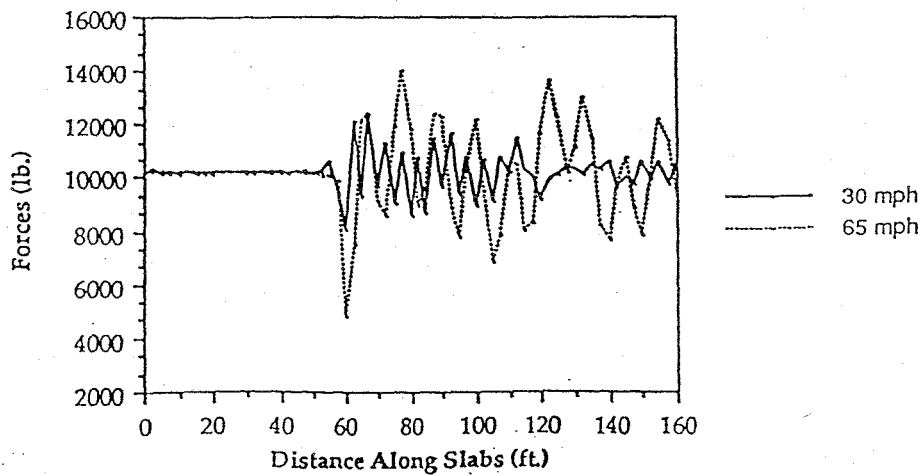


Figure 31 (c)
Dynamic Wheel Path Load for Trailing Axle of Tractor Tandem
(half inch fault)

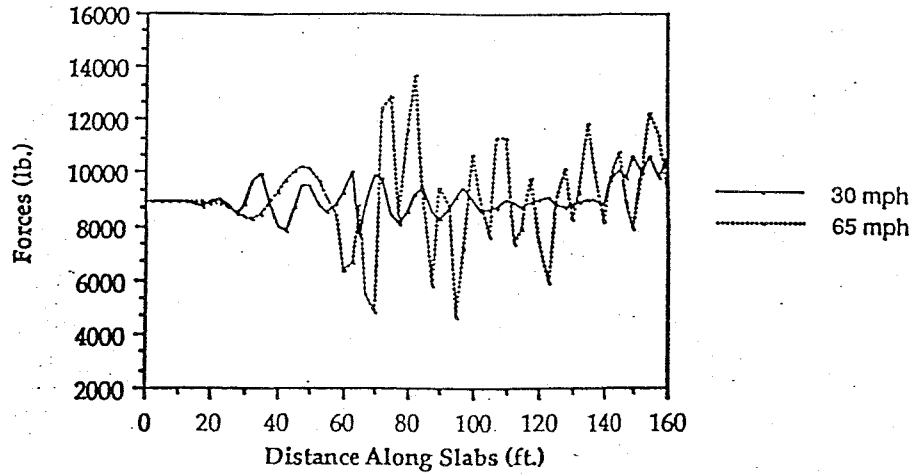


Figure 31 (d)
Dynamic Wheel Path Load for Leading Axle of Semitrailer Tandem
(half inch fault)

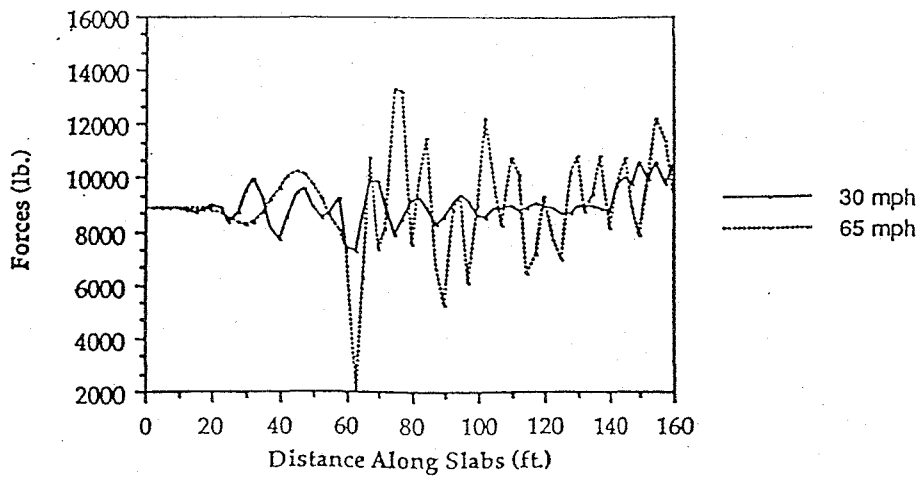


Figure 31 (e)
Dynamic Wheel Path Load for Trailing Axle of Semitrailer Tandem
(half inch fault)

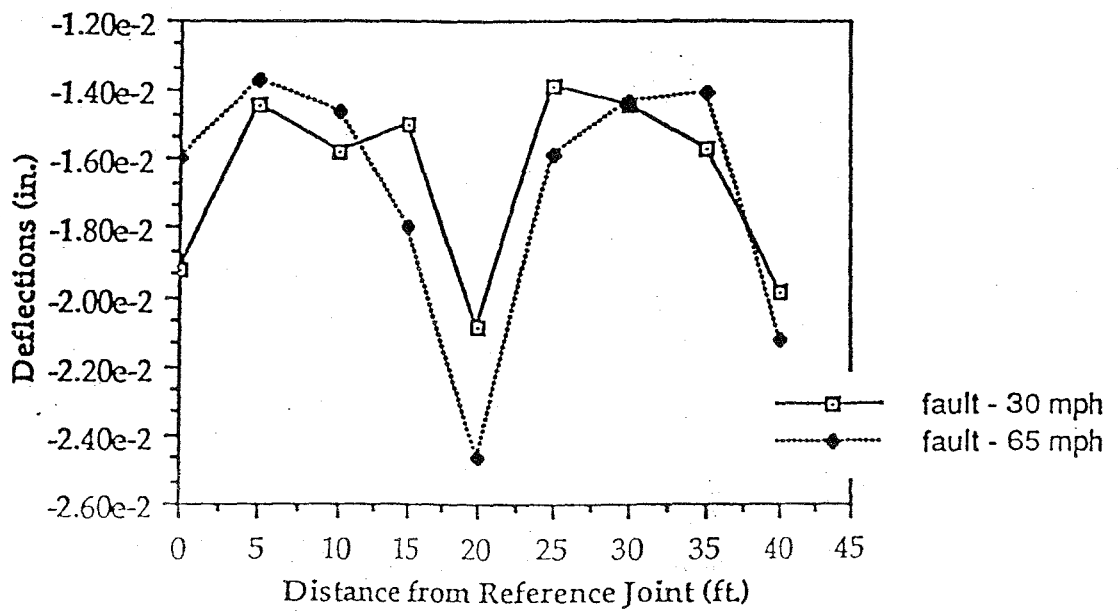


Figure 32
Envelope of Maximum Slab Displacement for Faulting Case

produces larger deflections. The overall envelope pattern is similar in both the bump and fault cases.

4. Results for 1/4 inch continuous fault case

Each 20 foot segment of the pavement is assumed to have a 1/4 inch fault. Thus the overall appearance of the model pavement is similar to a saw tooth. Axle forces were computed for three different speeds, namely, 30 mph, 45 mph, and 65 mph. The dynamic simulation was carried out for a duration adequate to obtain a nearly steady state response. The dynamic forces at the axles, shown in Figures 33(a)-(e), are taken from the steady state section of the results. The force records for the steering and the tractor axles show the effect of higher frequencies, however, those for the semitrailer axle show essentially a single frequency response. This single frequency corresponds to the pitch mode of the semitrailer. The 45 mph case is clearly dominant as far as the semitrailer axles are concerned. This can be directly attributed to the fact that the slab segments are 20 feet long, causing a resonance effect with the 45 mph speed. The maximum displacement envelope is shown in Figure 34. The envelopes are similar to the constant force case of applied static loads shown in Figure 35 indicating that the steady state dynamic effects are not very significant for this case. As expected, the joints experience the largest deflections for all speeds, with the 45 mph case again being the dominant one.

5. Results for 1/4 inch continuous warp case

Each 20 foot segment of the pavement is assumed to be warped into a "dish" shape with a 1/4 inch depth. This case is designed to simulate a long stretch of pavement exhibiting slab warp. Axle forces were computed for the three different speeds, namely, 30 mph, 45 mph, and 65 mph. A nearly steady state response was again obtained. The dynamic forces at the axles, shown in Figures 36(a)-(e), are taken from the steady state segment of the results. Just as in the case of continuous fault case, the force records for the steering and the tractor axles show the effect of higher frequencies, with the semitrailer axle showing a single frequency response with the 45 mph case clearly dominant. This can again directly be attributed to the slab segment being 20 feet long causing the resonance effect with the 45 mph speed. The maximum displacement envelope is shown in Figure 37. The envelopes show that the dynamic effects are significant for this case. As expected, the joints experience largest deflections for all speeds, with the 45 mph case remaining dominant.

Among all the cases studied, the continuous warp case is clearly the most interesting. It is also close to an actual rough pavement as observed from profilometer records. Thus this case is selected for investigation of the effect of pay load on the response of the pavement. The 45 mph case is repeated with the pay load reduced to two-thirds and one third the maximum, and then to the empty trailer condition and 0. The response envelopes are shown in Figure 38. These figures do not reveal anything extra ordinary other than confirmation of the fact that lighter loads produce smaller deflections. From a practical point of view a uniform reduction in pay load is not very interesting. A reduction in pay load, with different placement strategies in the truck, will be investigated in future.

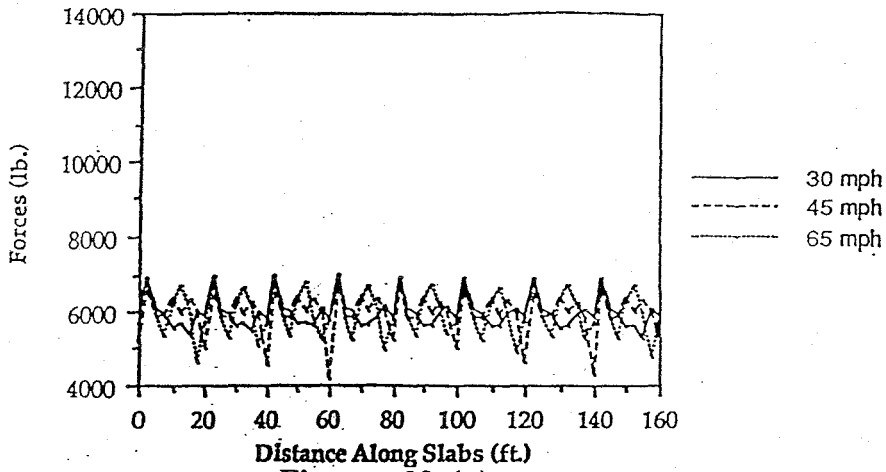


Figure 33 (a)
Dynamic Wheel Path Load for Steering Axle
(continuous faulting)

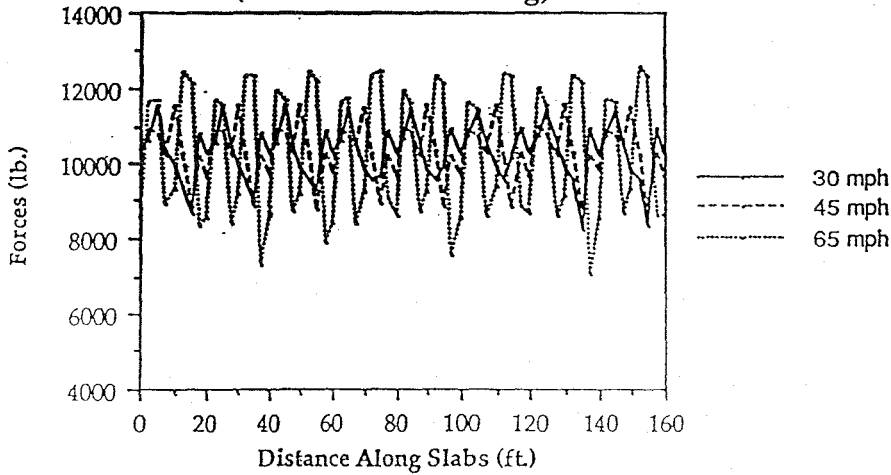


Figure 33 (b)
Dynamic Wheel Path Load for Leading Axle of Tractor Tandem
(continuous faulting)

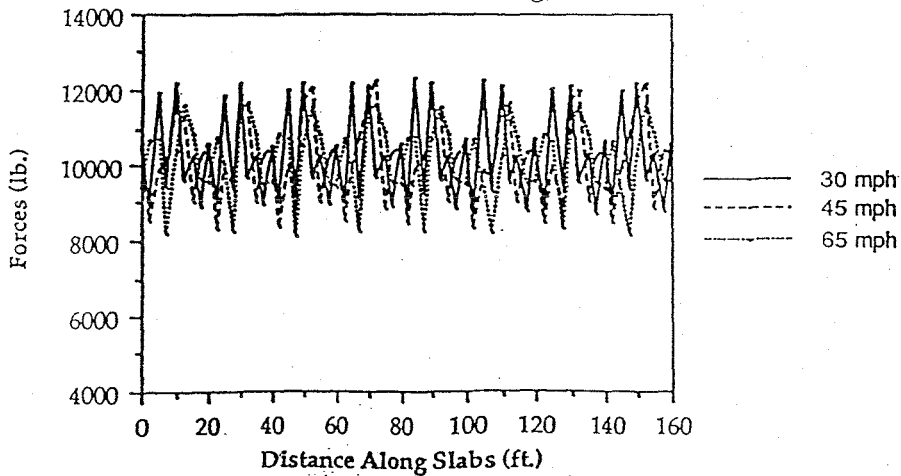


Figure 33 (c)
Dynamic Wheel Path Load for Trailing Axle of Tractor Tandem
(continuous faulting)

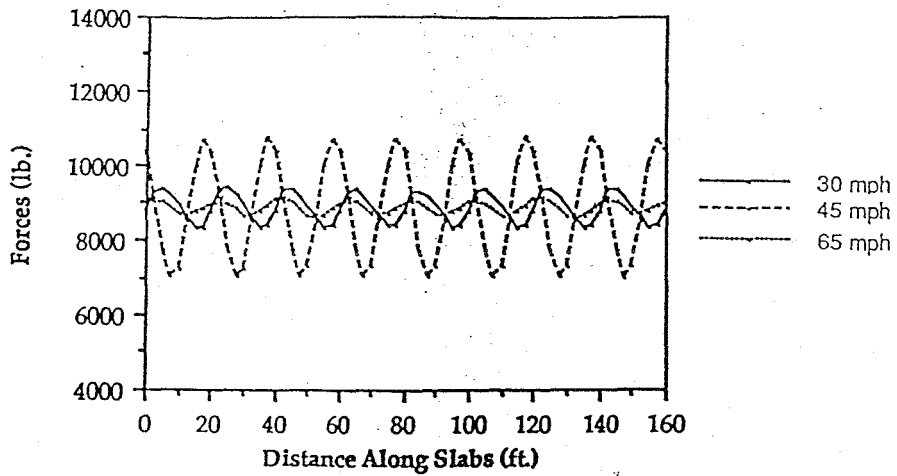


Figure 33 (d)
Dynamic Wheel Path Load for Leading Axle of Semitrailer Tandem
(continuous faulting)

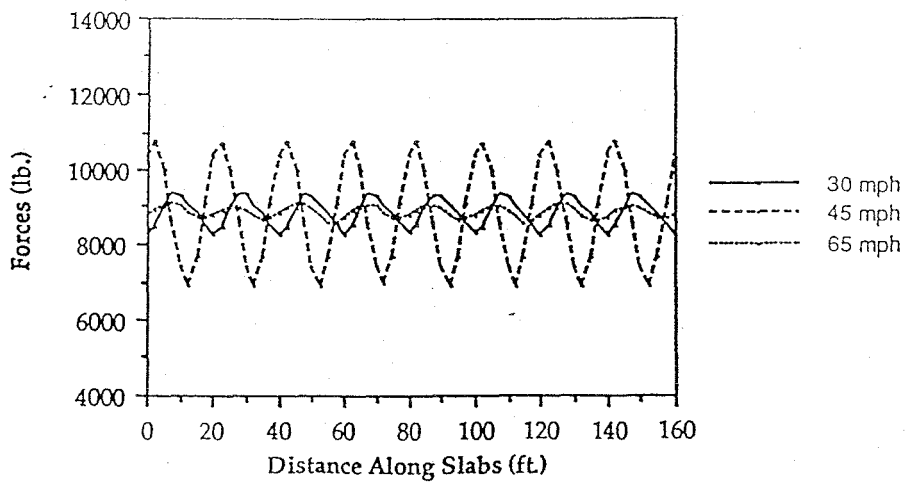


Figure 33 (e)
Dynamic Wheel Path Load for Trailing Axle of Semitrailer Tandem
(continuous faulting)

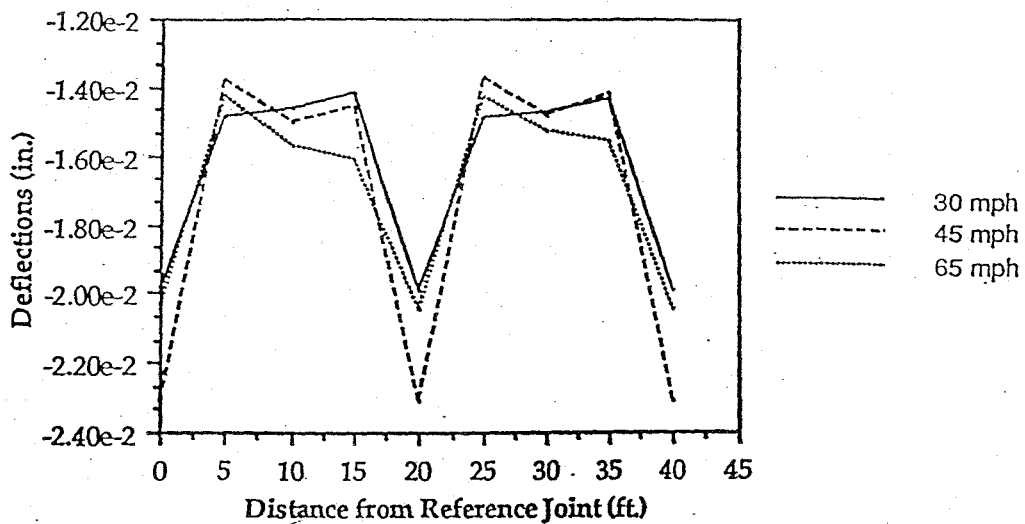


Figure 34
Envelope of Maximum Slab Displacements for Continuous Faulting Case

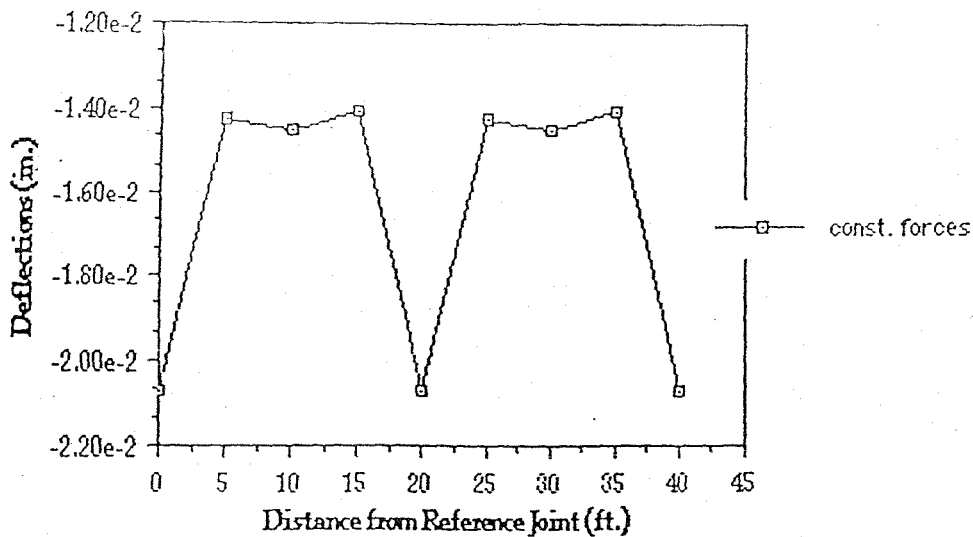


Figure 35
Envelope of Maximum Slab Displacements for Moving Static Load

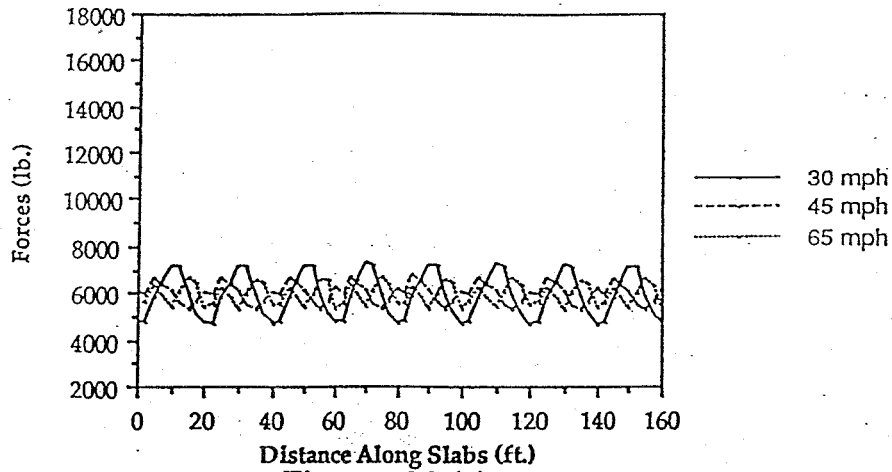


Figure 36 (a)
Dynamic Wheel Path Load for Steering Axle
(continuous warping)

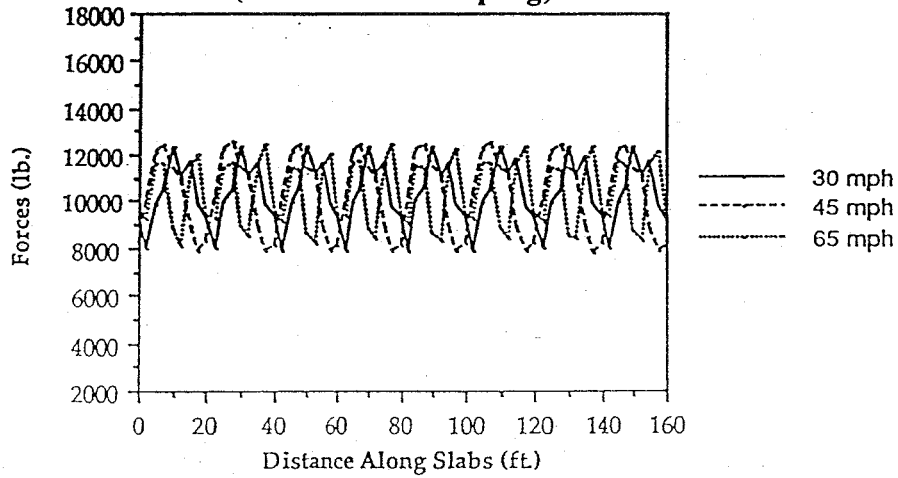


Figure 36 (b)
Dynamic Wheel Path Load for Leading Axle of Tractor Tandem
(continuous warping)

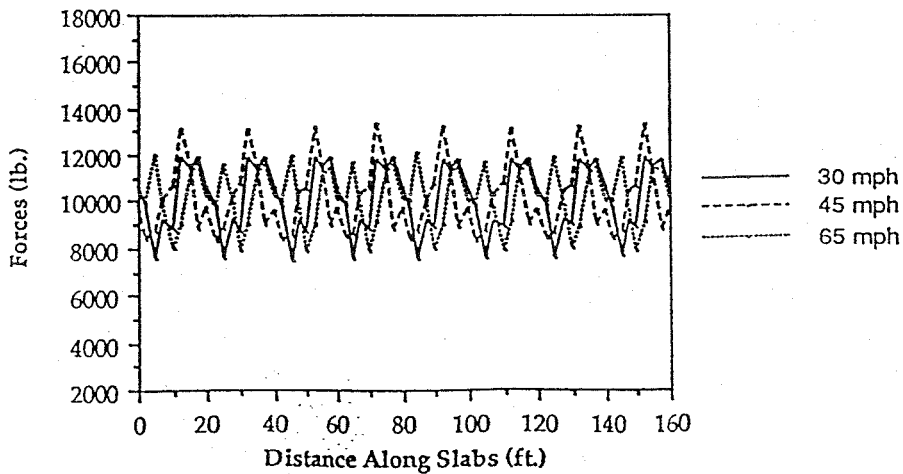


Figure 36 (c)
Dynamic Wheel Path Load for Trailing Axle of Tractor Tandem
(continuous warping)

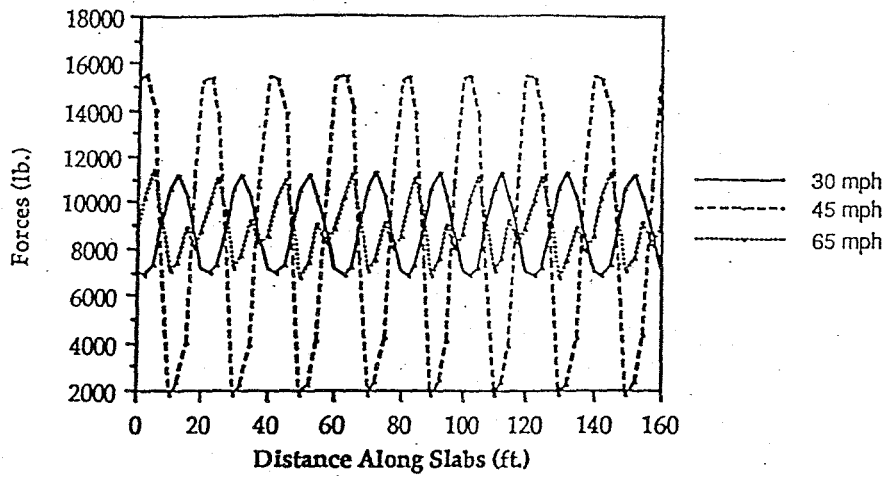


Figure 36 (d)
Dynamic Wheel Path Load for Leading Axle of Semitrailer Tandem
(continuous warping)

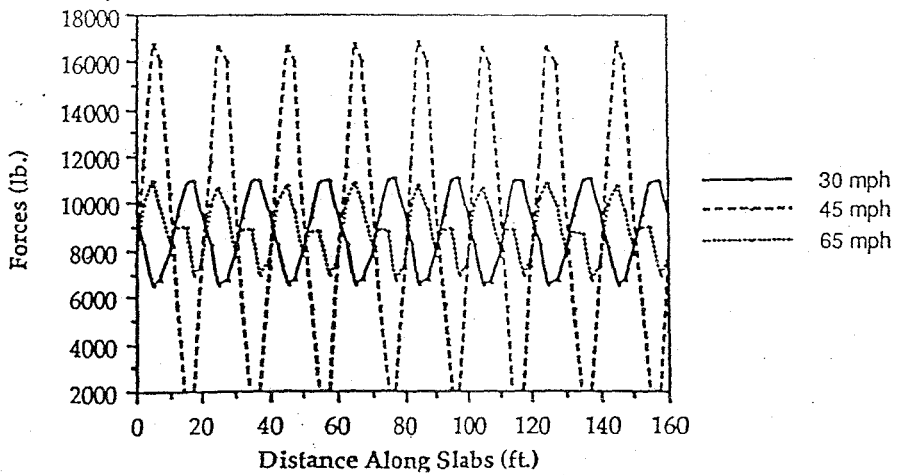


Figure 36 (e)
Dynamic Wheel Path Load for Trailing Axle of Semitrailer Tandem
(continuous warping)

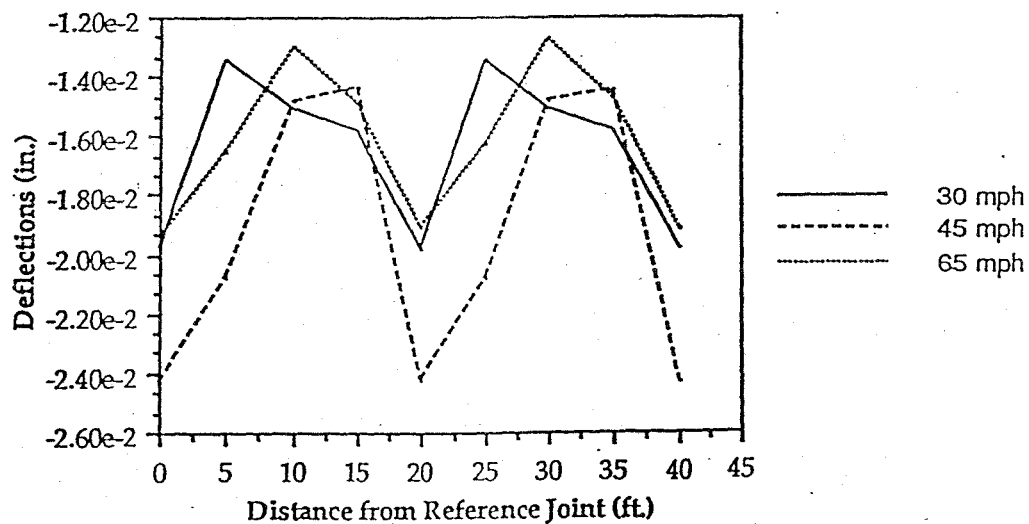


Figure 37
Envelope of Maximum Slab Displacements for Continuous Warp Case

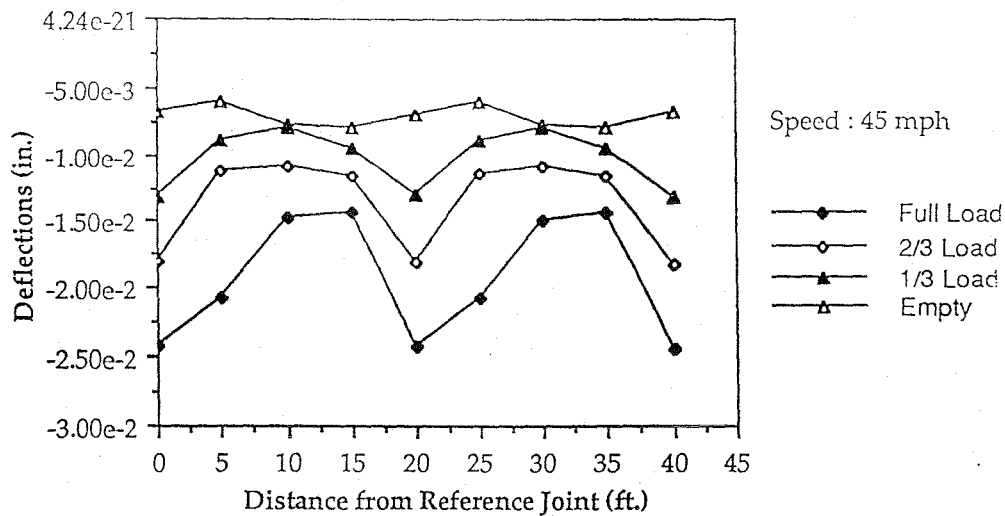


Figure 38
Pay Load Effect of Trailer on Slab Displacement Envelope

6. Results for actual I-80 profile case

Dynamic simulation was carried out using actual profilometer data from the Iowa Department of Transportation test site near Avoca, Iowa. Axle forces were computed for 30 mph and 65 mph. The dynamic forces at the axles are shown in Figures 39(a)-(e). The force records show considerable dynamic effects for 65 mph case. The maximum displacement envelope is shown in Figure 40. The envelopes again show that the dynamic effects are significant for the 65 mph case and are extremely variable because of the transient conditions. The joints experience largest deflections for all speeds.

7. Axles Causing Maximum Deflections

Table 2 contains information about the axle which causes maximum deflection of all cases studied for this report. The sequential axle number (the steering axle called number 1) that causes maximum deflection at the start of segment, middle of segment, and at the end of the segment is identified. This information is important in qualitatively studying the axle force histories and deflection envelopes. In essentially all cases when the truck is fully loaded, the maximum deflection at the joints occurs when the 5th axle is passing over that joint. For the middle of the slab, the maximum displacement usually occurs when the third axle is passing over that point.

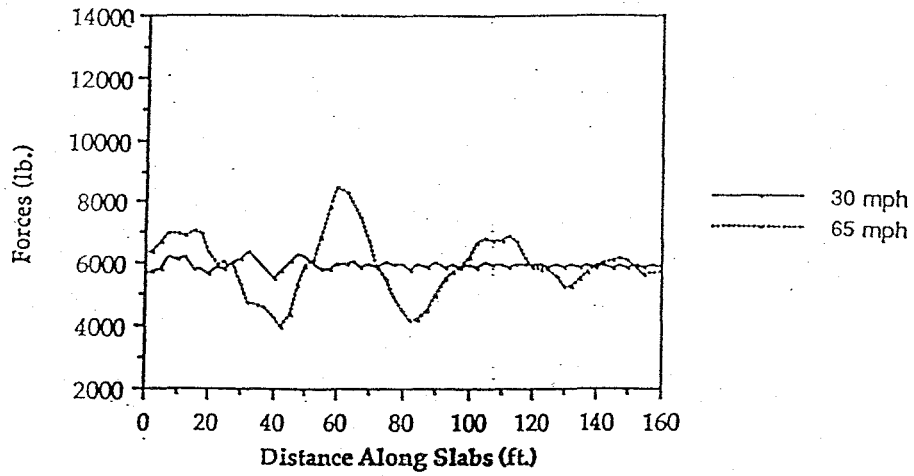


Figure 39 (a)
Dynamic Wheel Path Load for Steering Axle
(real profile)

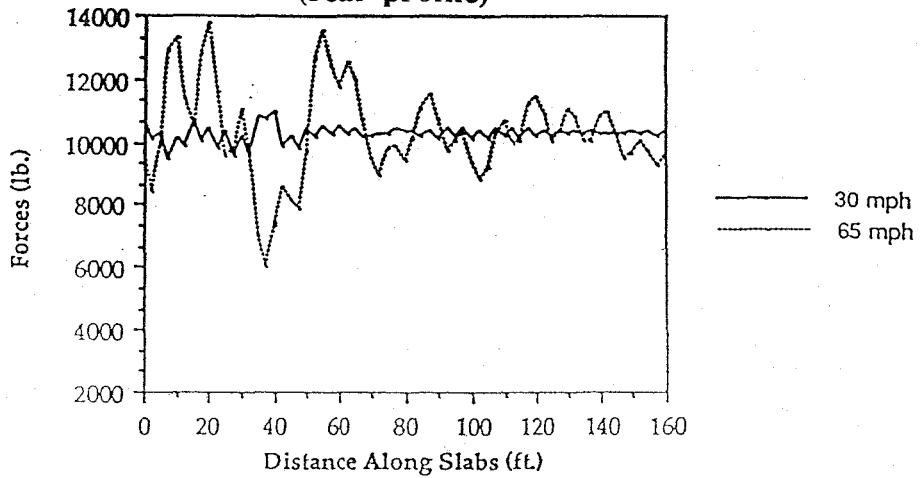


Figure 39 (b)
Dynamic Wheel Path Load for Leading Axle of Tractor Tandem
(real profile)

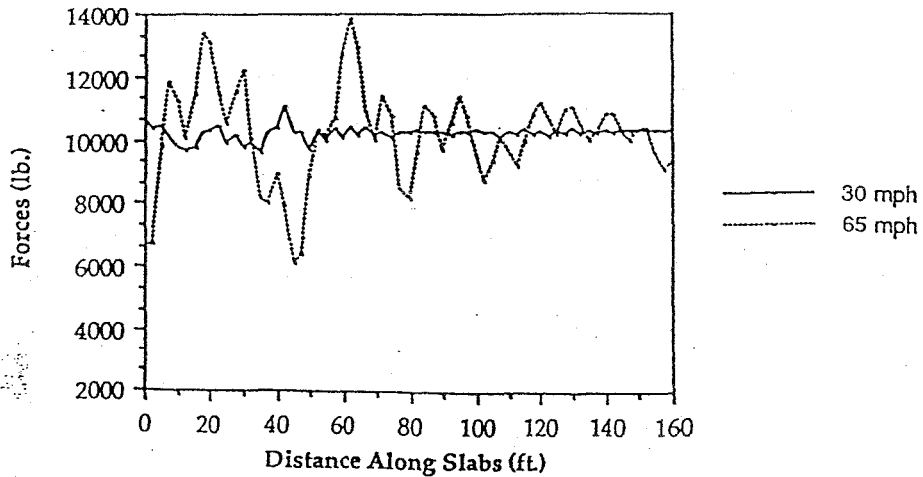


Figure 39 (c)
Dynamic Wheel Path Load for Trailing Axle of Tractor Tandem
(real profile)

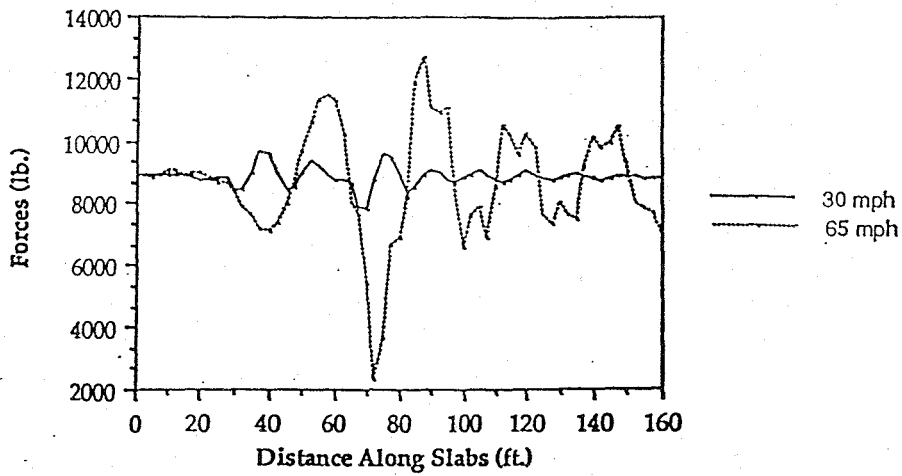


Figure 39 (d)
Dynamic Wheel Path Load for Leading Axle of Semitrailer Tandem
(real profile)

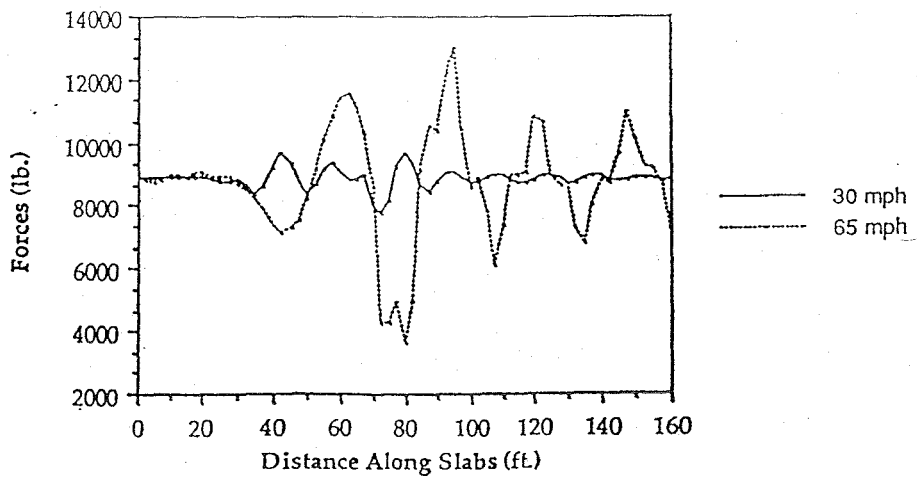


Figure 39 (e)
Dynamic Wheel Path Load for Trailing Axle of Semitrailer Tandem
(real profile)

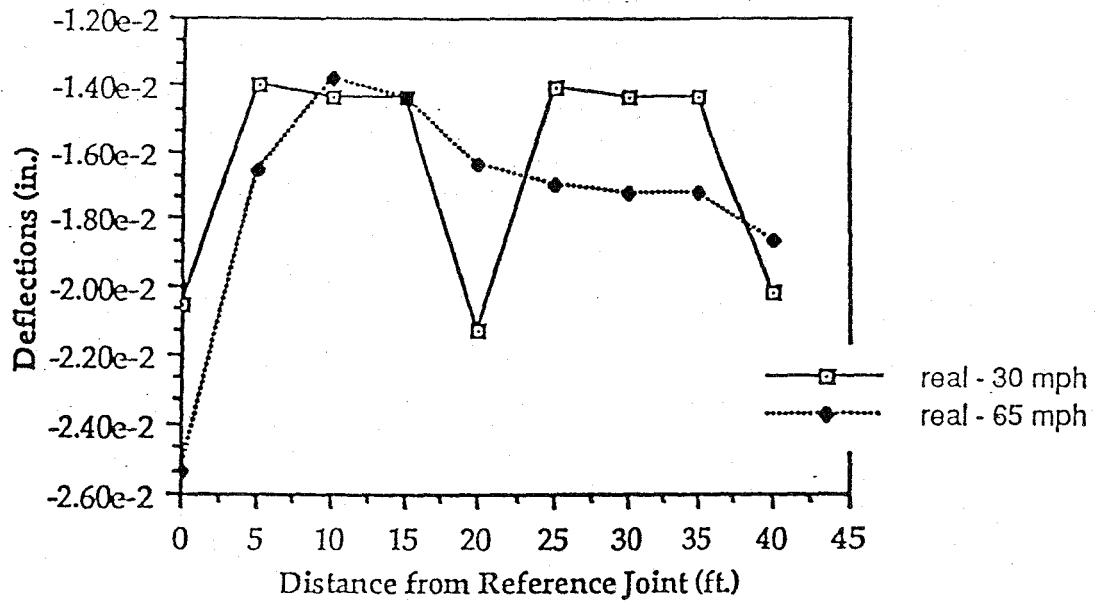


Figure 40
Envelope of Maximum Slab Displacements for Real Profile Case

Table 2
Axles Causing Maximum Deflections at Different Locations
and Different Road Conditions

	Start Slab I	Middle Slab I	End Slab I	Start Slab II	Middle Slab II	End Slab II
Bump - 30 mph	5 th	3 rd	5 th	5 th	5 th	5 th
Bump - 65 mph	5 th	3 rd	5 th	5 th	5 th	5 th
Fault - 30 mph	5 th	5 th	5 th	5 th	3 rd	5 th
Fault - 65 mph	5 th	5 th	4 th	4 th	3 rd	5 th
Real - 30 mph	5 th	3 rd	5 th	5 th	3 rd	5 th
Real - 65 mph	5 th	3 rd	3 rd	3 rd	5 th	5 th
Const. Forces	5 th					
Cont. Fault - 30 mph	5 th	3 rd	5 th	5 th	3 rd	5 th
Cont. Fault - 45 mph	5 th	3 rd	5 th	5 th	3 rd	5 th
Cont. Fault - 65 mph	5 th	3 rd	5 th	5 th	3 rd	5 th
Cont. Warp - 30 mph	5 th					
Cont. Warp - 45 mph	5 th	3 rd	5 th	5 th	3 rd	5 th
Cont. Warp - 65 mph	5 th					
Cont. Warp-45mph-Emp.	1 st	3 rd	1 st	1 st	3 rd	1 st

RESEARCH DISCUSSION

The second year of research will build on the results of the first year's work. A considerable amount of the first year effort was spent reviewing past research efforts and developing appropriate vehicle and pavement models that produced the required information. The second year will involve more parameterization and the development of integrated computer packages that lend themselves to policy analysis.

Summary of First-Year Findings

A number of lessons were learned during initial phase of the research. It was found that considerable research had been performed in an attempt to discern the magnitude of dynamic loads on pavement and relative pavement damage. The various studies had quite different objectives and the results were not always generalizable, or of aid to further studies. The prediction of loads was often performed with very simplified vehicle models that would tend to under-estimate the effects of the unsprung mass. Studies have often not relied on realistic roadway descriptions to the vehicle model. Some excellent studies have been completed, or are on-going, and the over-all level of research competence seems to be quite good.

A good description of the geometry, physical characteristics, and response relationships for the component parts of the vehicles is not readily available. The data used for many of the studies has produced erroneous load predictions. Much of the data is considered to be proprietary by the manufacturers, although some is available through the data base for the Phase Four program at UMTRI. Appropriate modeling does require the results from a test facility where the trailer and tractor are disassembled and the component parts physically measured and tested.

Models of pavement response are anything but precise, and perhaps only reliable over a specific range of parameter values. Each section of pavement can be quite different, even though associated with the same pour. Falling Weight Deflectometer studies show considerable differences in back calculated soil support values over very short distances of the same segment of newly constructed highway. Much more longitudinal data collection from instrumented pavements located in a variety of soil and traffic conditions needs to be collected to support changes in pavement thickness and geometric design procedures.

Some very preliminary findings from our study would lead to the following conclusions

- (1) Pavement that is assumed to be smooth and having a low value of road roughness measure in inches per mile, can produce some significant (10-15 percent) increases in wheel path impact loadings.
- (2) Smooth, tangent sections of pavement usually produce dynamic load coefficients less than 1.05.
- (3) Dynamic loads may be of considerable importance in the design of urban arterial streets where the performance standards for road roughness of new construction are much lower.

- (4) Higher speeds generally produce higher transient values of peak impact load.
- (5) Steady state conditions on road having considerable regular slab faulting and slab warping can result in extremely high dynamic loads for the rear tandem axle set because of the excitation of the unsprung mass modes at critical speeds. The location of the peak impact loads on the slabs is a function of axle spacing, speed, and slab length.
- (6) Initial pavement quality may be very important in determining the pavement life and eventual damage and deformation caused by load replications. The irregular damage from pavement failure may not be as important if adequate maintenance standards are in place.
- (7) Dynamic load coefficients are usually higher for the semi-trailer tandem axle for a loaded vehicle, but the steering axle causes the greatest pavement deformation for a lightly loaded or empty vehicle
- (8) Potential pavement damage needs to be a criterion when considering alternative truck combinations.
- (9) Vertical geometry and continuity of the pavement may be a more significant factor in design life than interim damage from axle replications.
- (10) Study of true cost of vehicle pavement damage needs to be related to the efficiency and productivity of the vehicles. Some bridge formula interpretations may be too limiting.

Further Research Needs

A number of research needs for state Department's of Transportation and other facility design and operating authorities, seems to be implied by the first year findings.

1. A more appropriate method of measuring pavement roughness and sufficiency need to be developed to allow construction contract monitors and maintenance programmers a better indicator of potential problems resulting from high levels of truck traffic. Profilometer data can be interpreted a number of ways and do not take into account the lower frequency variations that can cause more problems than intermittent peaks.
2. Digital data on longitudinal profilometer data needs to be available for analysis with vehicle dynamics programs and other post processors to determine appropriate statistics for structural adequacy of the pavement.
3. Long term monitoring of instrumented pavement projects needs to be initiated at the earliest opportunity at the state level. The technology for remote monitoring and procedures for appropriate installation have been developed during the past few years. Every new project should be considered for implementation, especially if a significant number of heavy axle load replications is predicted.

4. Alternative Vehicle Configurations should be evaluated with respect to both peak impact loads and inherent vehicle stability as part of the licensing and classification procedures. This is especially true for some of the more experimental trailer combination and special purpose rigs. Each and every vehicle is likely to be different with respect to response to roadway imperfection and the resulting effect on roadway life. It would be impossible to come up with enough vehicle classifications to take all factors into account, but a reward structure should be developed for the implementation of improved suspensions, tires, axle sets, and trailer design.

5. Alternative pavement designs that attempt to extend service life should be evaluated with a modeling process and validation procedure initiated for long term evaluation. The same is true for pavement rehabilitation practices such as full joint replacement, and grinding and smoothing of pavement surfaces.

6. Longitudinal, time series data should be collected to record variation in soil support values resulting from changes in temperature, moisture content, and construction practice. Improved finite element models can be used to determine the importance of various soil stabilization techniques and the use of aggregate sub-bases for rigid pavement.

Proposed Research Extensions and Second Year Work Plan

The proposed work tasks for the second year of work on this project will address many of the research questions raised in this report and build on the products of the first year.

Work has started on implementing a three dimensional, recursive dynamics code that will allow real time simulations and animation. This will allow evaluation of situations where wheel loadings are not uniform across the pavement because of skewed joints or vehicle maneuvers.

A specific dynamic simulation code is being developed for modeling only alternative configurations of heavy trucks. This two dimensional model will allow the instantaneous analysis of existing or proposed vehicles by assembling modules representing axle sets, trailers, suspension types, etc.

A plate model for pavement evaluation is being integrated with the finite element code to allow the analysis of accrued weakening of the pavement and associated plastic deformation and slab cracking. Damage functions will be tested to evaluate estimates of service life and life cycle cost of the pavement.

Extensive parameterization of alternative vehicle designs will provide data for determination of what factors are critical in determining the magnitude of peak impact loads.

Data from the instrumented pavement will be evaluated in the Spring of 1990 to determine the appropriate scales to use for deflection data collected from the site. The results from the strain gauges will be utilized to verify the performance of the finite element programs.

The specifications for integrating the vehicle dynamics code and the finite element pavement analysis will be determined and the appropriate interface defined. The intent is to develop a product that will be useful in policy analysis and the evaluation of site specific pavement designs.

REFERENCES

- Bae, D.S. and Haug, E.J., "A Recursive Formulation for Constrained Mechanical System Dynamics," Technical Report 86-14, Center for Computer Aided Design, The University of Iowa, Iowa City, Iowa, 52242.
- Cebon D. "Theoretical road damage due to dynamic tyre forces of heavy forces of heavy vehicles Part 1: dynamic analysis of vehicle and road surfaces" IMechE Vol. 202 No C2 pp. 103-108.
- Cebon D. "Theoretical road damage due to dynamic tyre forces of heavy vehicles Part 2: simulated damage caused by a tandem-axle vehicle," IMechE Vol. 202 No C2 pp. 109-117.
- Chou, Y.T., Structural Analysis Computer Programs for Rigid Multicomponent Pavements Structures with Discontinuities - WESLIQID and WESLAYER. Reports 1, 2 and 3. U.S. Army Engineer Waterways Experiment Station, Miss, May 1981.
- "DADS User's Manual, Rev. 5.0" Computer Aided Design Software Inc., Jan. 1988.
- Markow M.J., et al "Analyzing the interactions between dynamic vehicle loads and highway pavements" submitted to Transportation Research Board Washington, D.C. March, 1988.
- Morris J.R. "Effects of Heavy Vehicle Characteristics on Pavement Response and Performance - Phase 1," National Cooperative Highway Research Program, Transportation Research Board, Dec. 1987.
- Sayers M. and T.D. Gillespie "Dynamic Pavement/Wheel Loading for Trucks with Tandem Suspensions," Proceedings of the 8th IAVSD Symposium, 1983.
- Ullidtz, Per. Pavement Analysis, Elsevier, New York, 1987.

Appendix 1

The vehicle dimensions and parameters used in this model are listed as follows:

Tractor Parameters

Wheelbase-distance from front axle to the center of rear suspension (in)	138.0
Base vehicle curb weight on front suspension (lb)	10706
Base vehicle curb weight on rear suspension (lb)	5944
Sprung mass C.G. height (in)	42.1
Sprung mass pitch moment of inertia (in-lb-sec**2)	92522
Fifth wheel location (in. ahead of rear axle. center)	8.0
Fifth wheel height above ground (in)	42.6

Tractor front and axle parameters

Suspension spring rate (See Table A-1)	
Unsprung weight (lb)	1475

Tractor rear suspension and axle parameters

Tandem axle separation (in)	52
Suspension spring rate (See Table A-2)	
Unsprung weight of leading suspension (lb)	2550
Unsprung weight of trailing suspension (lb)	2310

Semitrailer parameters

Wheelbase-distance from kingpin to the center of rear suspension (in)	482
Sprung mass C.G. height (in. above ground)	74.8
Sprung mass pitch moment of inertia (in-lb-sec**2)	4336092

Semitrailer suspension and axle parameters

Tandem axle separation (in)	49.0
Suspension spring rate (See Table A-3)	
Unsprung weight of leading suspension (lb)	1530
Unsprung weight of trailing suspension (lb)	1530

Tire parameters

Tire stiffness (lb/in/tire)	4614
Tire loaded radius (in)	18.5

Static tire contact loads

Payload (lb fully loaded)	50426
Solid axle of tractor (lb)	11778
Leading tandem axle of tractor (lb)	20237
Trailing tandem axle of tractor (lb)	20033
Leading tandem axle of semitrailer (lb)	18105
Trailing tandem axle of semitrailer (lb)	18105

Table A-1 Front Axle Spring Rate

Compression Envelope

<u>Force (lb)</u>	<u>Deflection (in)</u>
-1200.0	-1.75
100.0	-0.75
100.0	-0.25
2050.0	1.00
8150.0	5.50
12650.0	8.25
25000.0	9.75

Extension Envelope

<u>Force (lb)</u>	<u>Deflection (in)</u>
-1200.0	-1.50
-100.0	-0.50
-100.0	-0.25
1450.0	1.00
5200.0	4.0
9000.0	6.88
12800.0	9.75

suspension deflection constant: 0.075 inches for compression
0.1 inches for extension

Table A-2 Tractor Tandem Axle Spring Rate

Compression Envelope

<u>Force (lb)</u>	<u>Deflection (in)</u>
-1150.0	-1.5
0.0	-1.2
300.0	-0.2
1000.0	0.0
2000.0	0.25
4800.0	1.0
8900.0	2.0
13200.0	3.0
24000.0	4.0

Extension Envelope

<u>Force (lb)</u>	<u>Deflection (in)</u>
-1150.0	-1.5
-200.0	-1.2
0.0	-0.2
400.0	0.0
1100.0	0.25
3600.0	1.0
7300.0	2.0
11000.0	3.0
15000.0	4.0

suspension deflection constant: 0.0125 inches for compression
0.025 inches for extension

Table A-3 Semitrailer Tandem Axle Spring Rate

Compression Envelope

<u>Force (lb)</u>	<u>Deflection (in)</u>
-121380.0	-11.0
-10525.0	-1.0
720.0	0.0
45120.0	4.0

Extension Envelope

<u>Force (lb)</u>	<u>Deflection (in)</u>
-122820.0	-11.0
-11820.0	-1.0
720.0	0.0
43680.0	4.0

suspension deflection constant: 0.05 inches for compression
0.05 inches for extension